Interaction of high flux plasma with Fe and RAFM steels: experimental and computational assessment

Dmitry Terentyev, Lorenzo Malerba, Athina Puype, Anastasia Bakaeva

SCK-CEN, Belgian Nuclear Research Centre

Outline

- Part I
  - Improving high-Cr grades
  - Mechanical data
- Part II
  - Exposure of pure Fe (in reference and deformed state)
  - Exposure of E97, T91 and two advanced grades
- Part III
  - Atomic-scale assessment of H in Fe
  - Computational model to consider Non-equilibrium trapping and its connection to diffusion limited trapping

Part I

Development of RAFM steels with advanced mechanical properties

Standard and improved high-Cr grades for Fusion Appl.

- One principle problem of 9-Cr steels: low temperature embrittlement
- Second one: creep, limiting application up to 650C

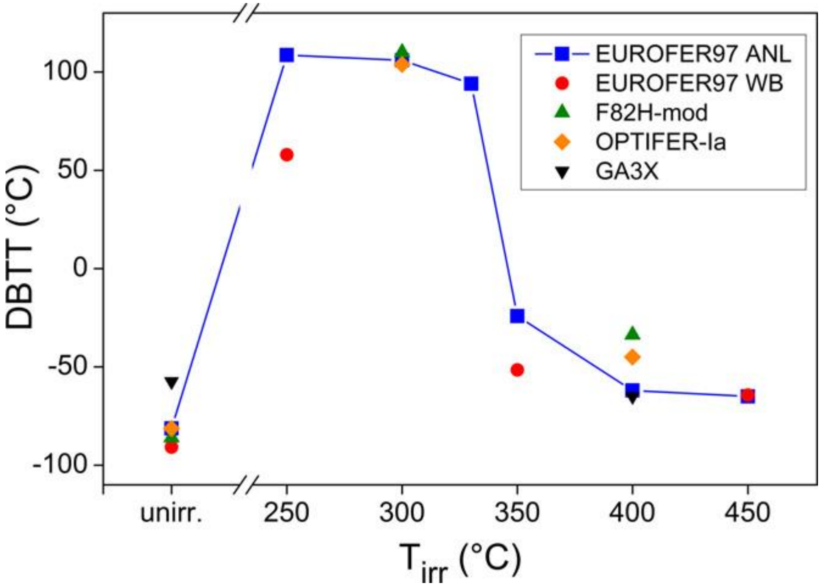

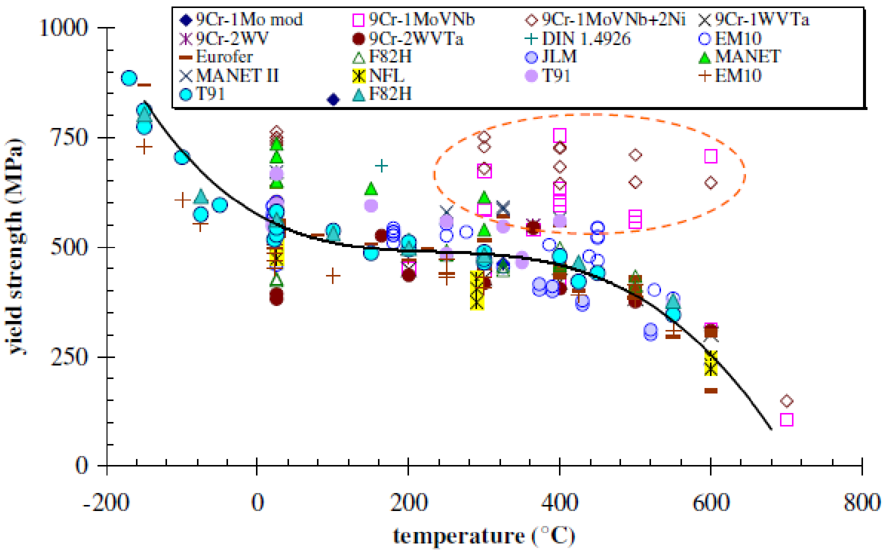

Steel	C	Si	Mn	Cr	Ni	Mo	W	V	Nb	B	N	Other
F82H	0.10	0.2	0.50	8.0			2.0	0.2		0.003		0.04 Ta
EUROFER	0.11	0.05	0.50	8.5			1.0	0.25		0.005		0.08 Ta

How to reduce DBTT and enhance creep resistance

- Modify precipitate distribution
  - Change ratio MC to MX
  - Modify H-treatment
  - Modify Composition
- V and Nb:
  - Stabilize grains
  - Reduce grain coarsening
  - Increase ductility
- Ta:
  - Carbide former & stabilizer
- 9Cr remains optimum
  - Less Cr – poor corrosion resistance
  - More Cr – hardening (α′) and δ-ferrite

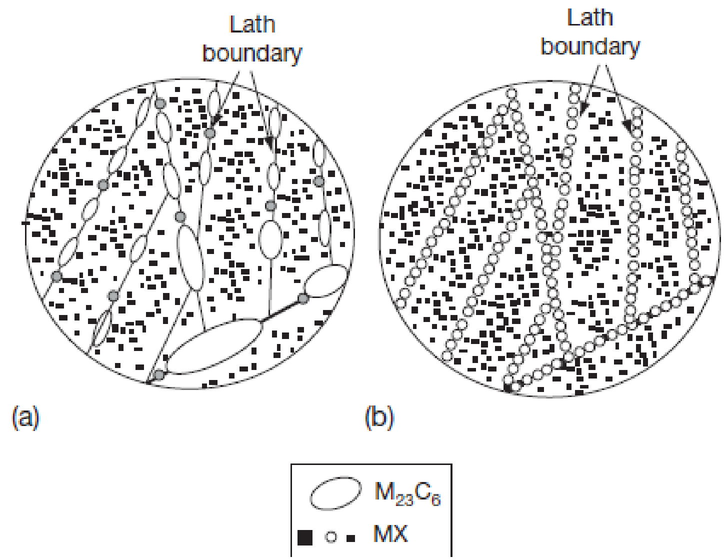

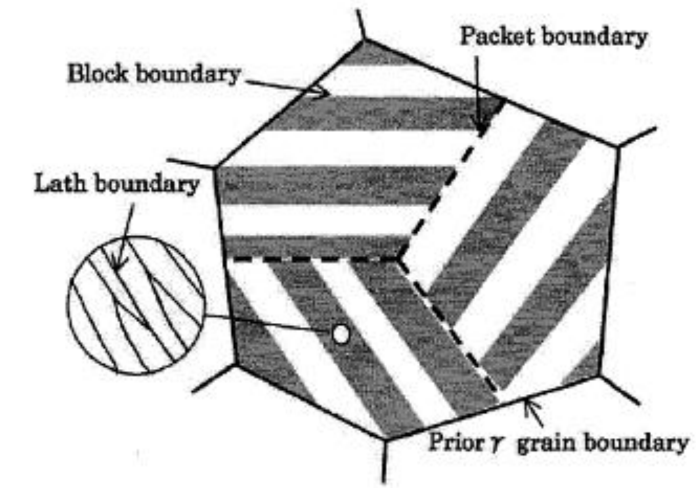

Advanced Thermo-Mechanical Treatment: TMT

0.09Ta

1

Pass 1		Pass 2		Pass 3		Pass 4		Pass 5		Pass 6	
T	%	T	%	T	%	T	%	T	%	T	%
1200	19.547	1150	25	1100	30	960	30	900	30	850	30

2

0.11Ta

Pass 1		Pass 2		Pass 3		Pass 4		Pass 5		Pass 6	
T	%	T	%	T	%	T	%	T	%	T	%
1220	21.978	1200	25	1180	30	1160	30	1140	30	1120	30

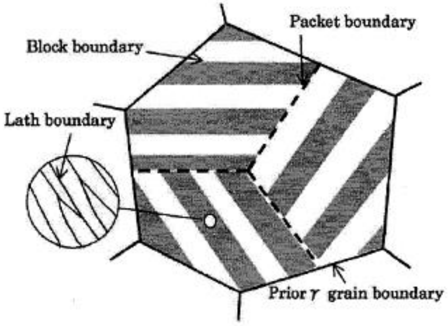

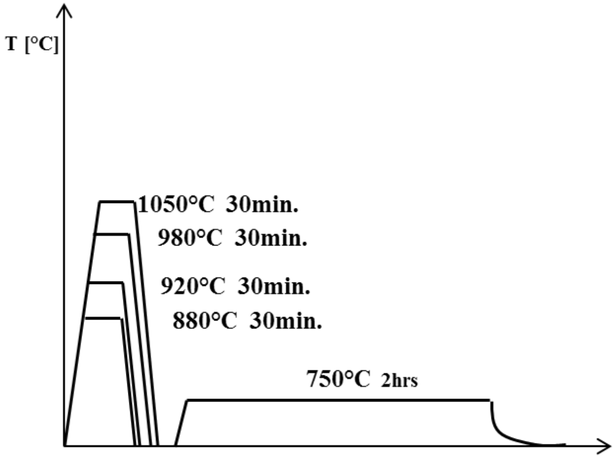

Effect of Heat Treatment

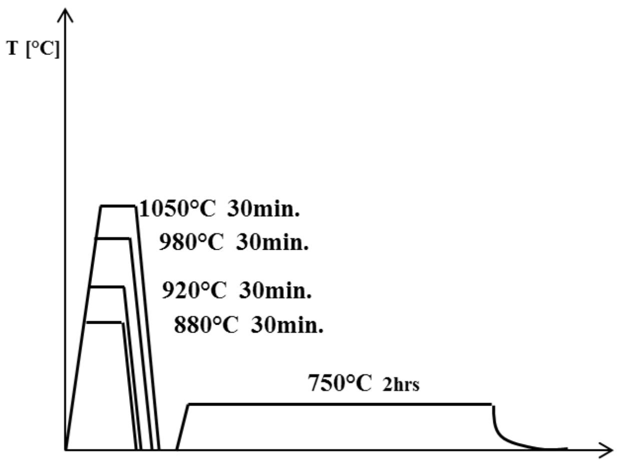

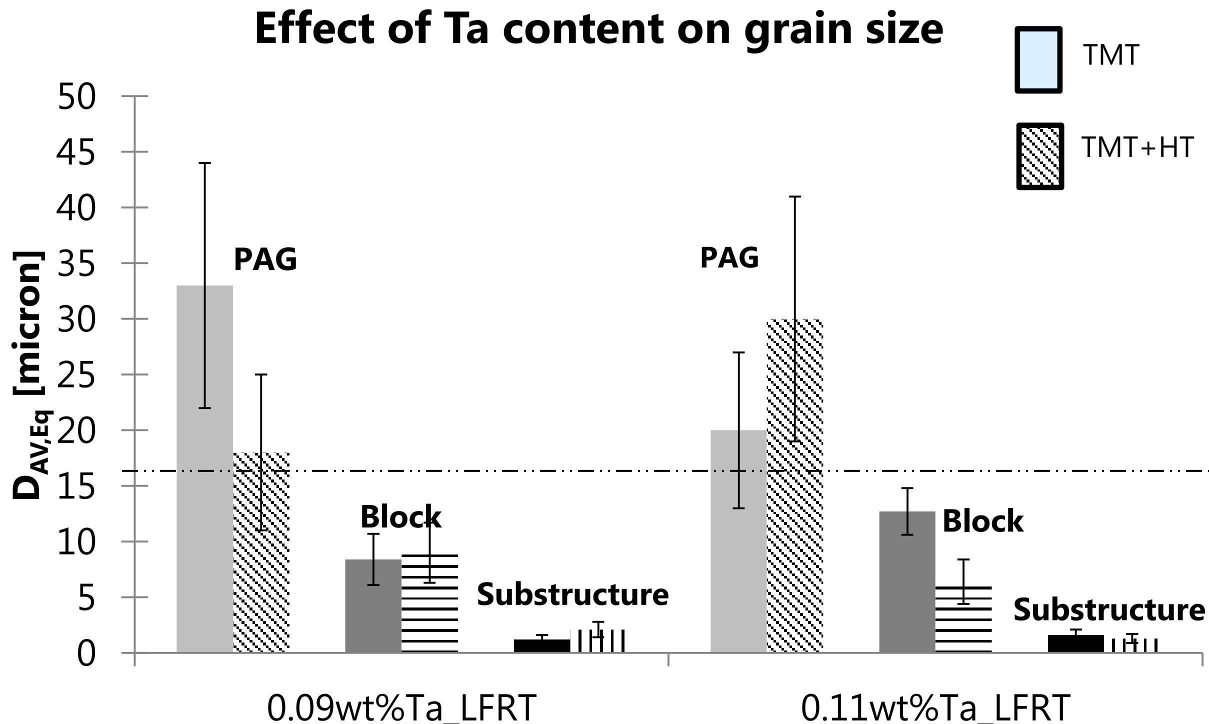

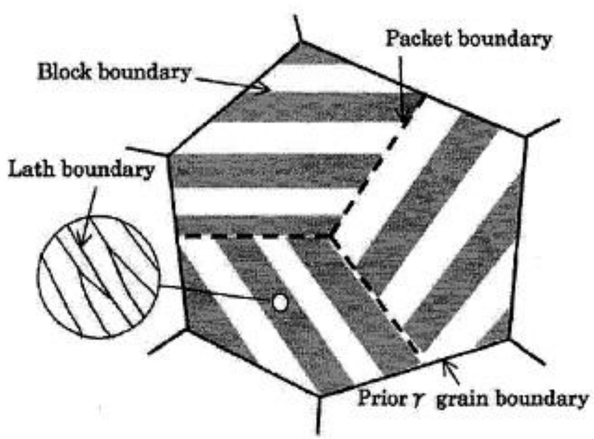

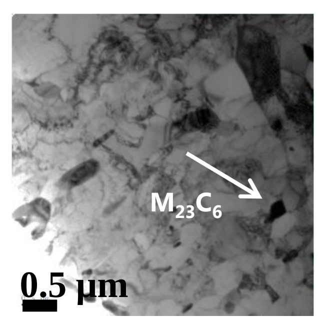

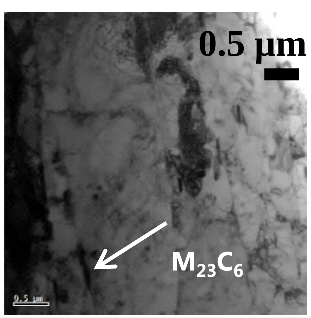

Role of heat treatment

Main differences after normalizing

880°C ➔ > dissolution temperature $M_{23}C_6$ **&** restriction prior austenite grain (PAG) growth by untransformed tempered martensite

after tempering : *small martensitic blocks with different degree of tempering and relatively large $M_{23}C_6$ mainly on packet boundaries*

920°C ➔ complete transformation to γ **&** homogeneously distributed carbon **&** hardly no PAG growth **&** high HAGB density

after tempering : *small martensitic blocks with smaller $M_{23}C_6$ on block and packet boundaries*

980°C ➔ > dissolution temperature MX **&** PAG growth

after tempering : *martensitic blocks with $M_{23}C_6$ more evenly distributed mainly on the block boundaries*

1050°C ➔ extended prior austenite grain growth **&** homogeneously distributed nitrogen **&** low HAGB density

after tempering : *relatively large martensitic blocks with elongated $M_{23}C_6$ on block and packet boundaries*

Precipitation of Vanadium and Tantalum

Fraction of elements that precipitate at different stages of Q&T treatment

Wt%	Cr	Ta	V
0.09Ta	9.3	0.086	0.22

wt%V & wt%Ta precipitated

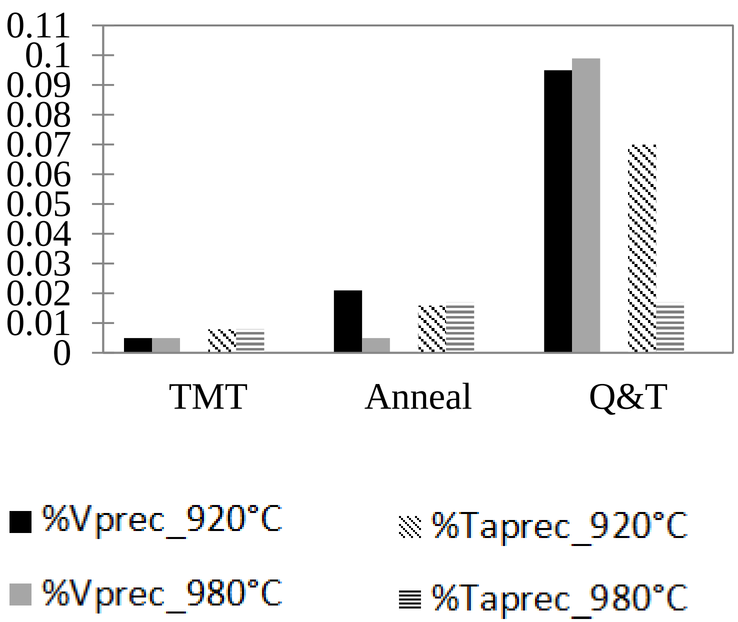

Martensite structure and carbide measurements

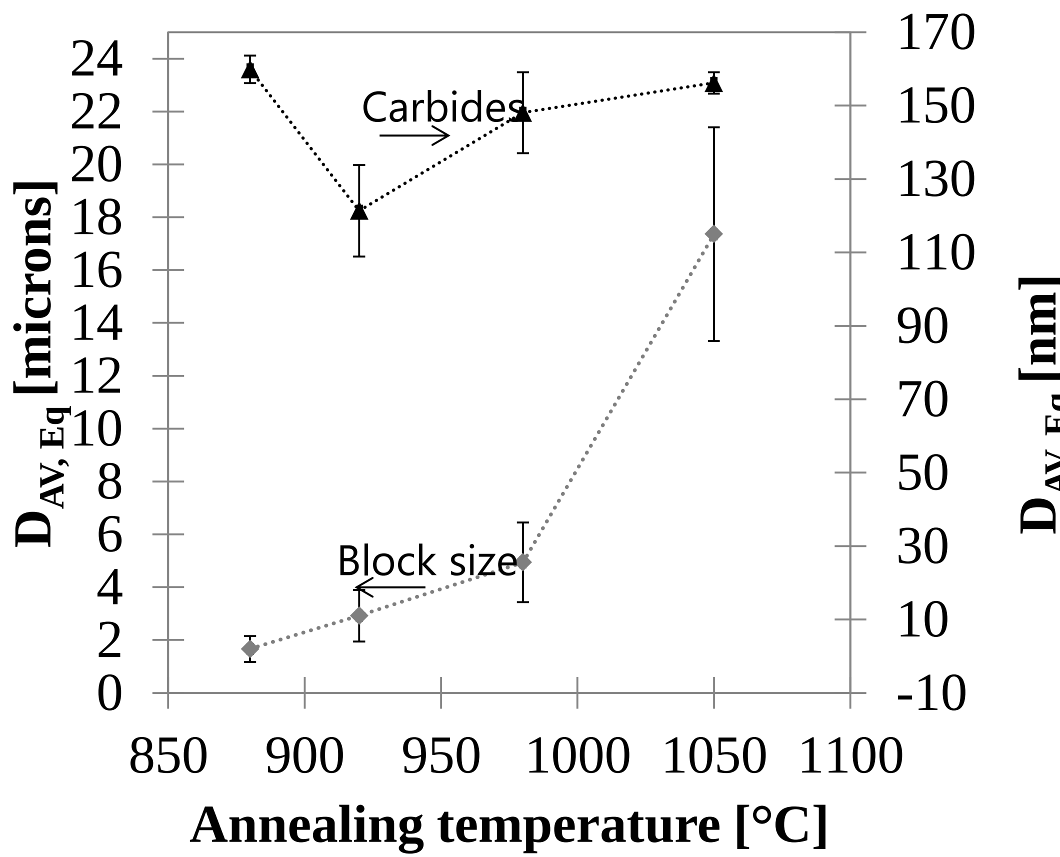

Mechanical properties of improved grades

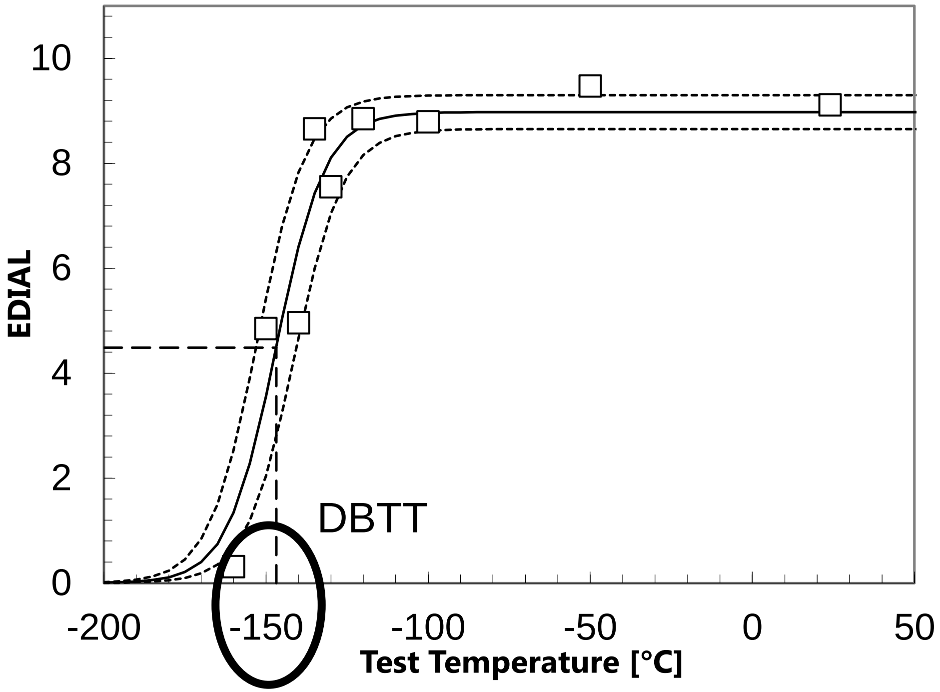

Q&T: 880°C tested at -140°C

Intermediate level

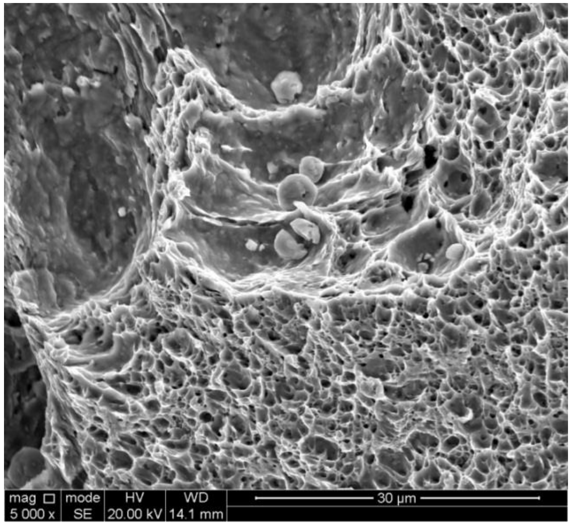

Two grades were selected for Plasma exposure

- "196C"
  - 0.11C;9Cr;1W;0.23V;0.09Ta;0.0113N;0.4 Mn;0.03Si
  - Heat treatment: 880°C 1/2h + water quench + 750°C for 2 hr.
  - low DBTT (-150C);
- "8Cr"
  - 0.02C;8Cr;1W;0.22V;0.13Ta;0.022N (No Mn&Si)
  - Heat treatment: 1050°C 1/4h + water quench + 675°C for 1.5h
  - Fine grain microstructure with; DBTT -90°C

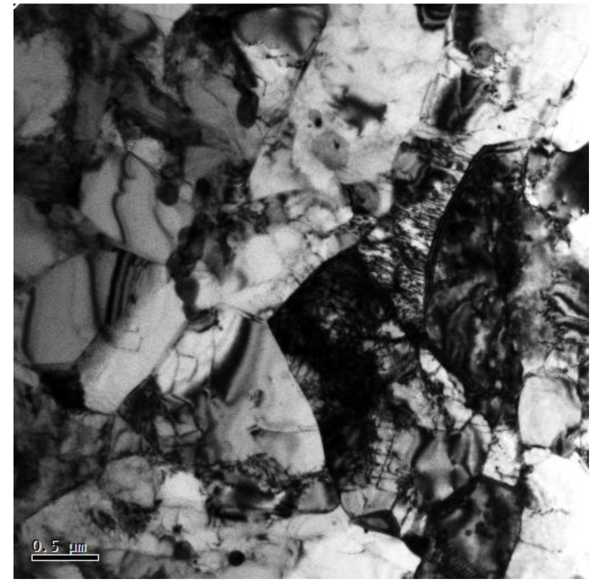

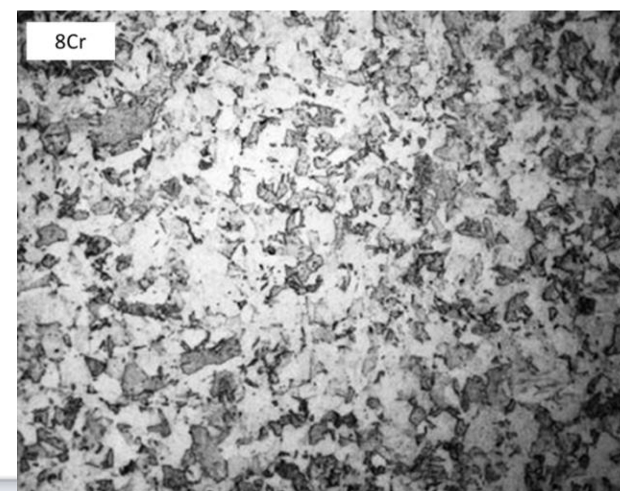

Part II

- Plasma exposure of pure Fe
- Plasma exposure of advanced RAFM and E97, T91

Depth distribution & sub-surface trapping

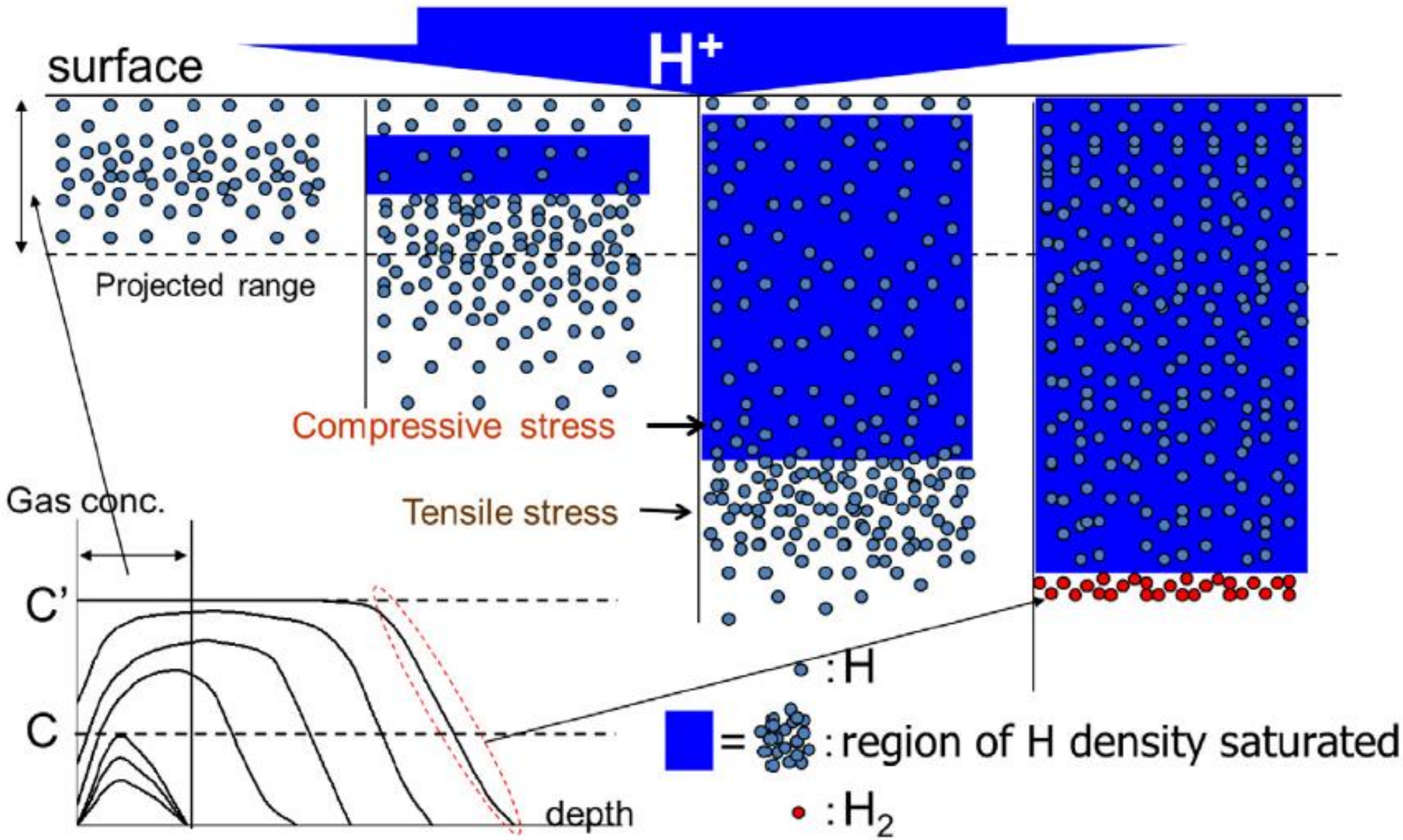

High heat flux plasma exposures

- PILOT-PSI (NL, DIFFER)
- Stationary Loads & ELM-like pulses
- B field = 0.4-1.6 T; target bias 50 eV
- Water cooling 20 C

(passive control of T surface)

- Flux 0.8×10^{24} D/m^2/sec

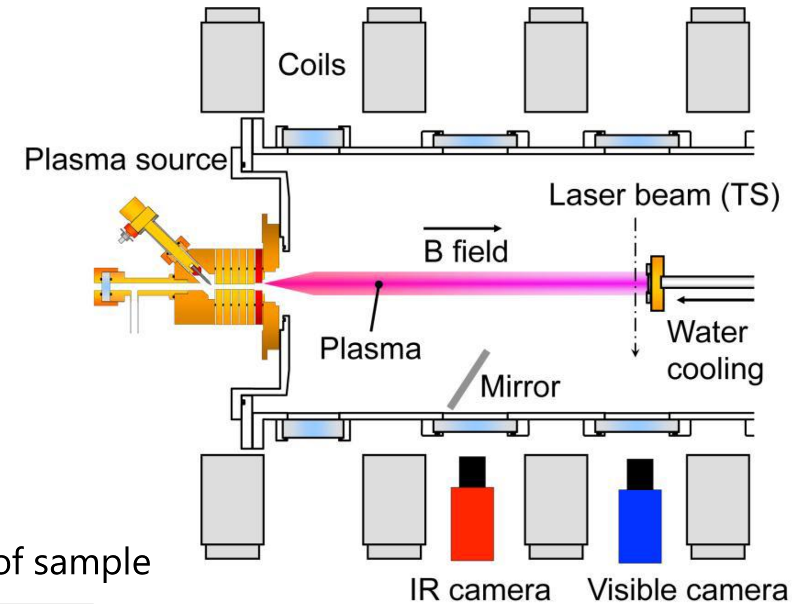

Temperature at the centre of sample

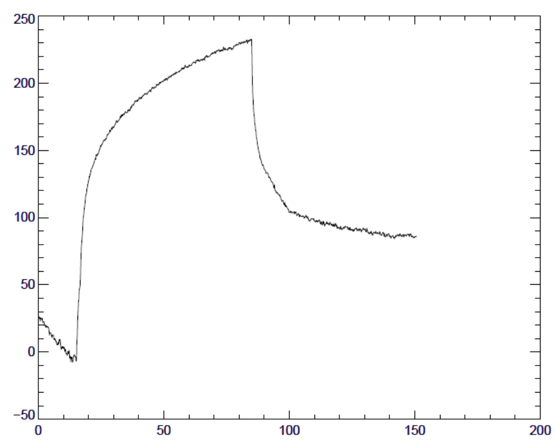

Typical ion flux profile

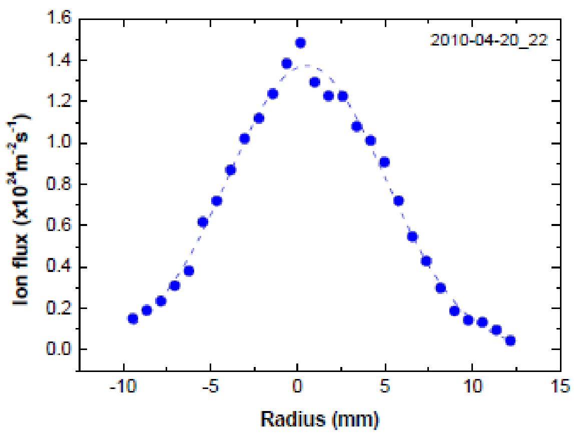

High flux plasma changes sub-surface

- Compressive stresses in sub-surface region generate:
  - Dense dislocation network
  - Limited within 10-15 μm

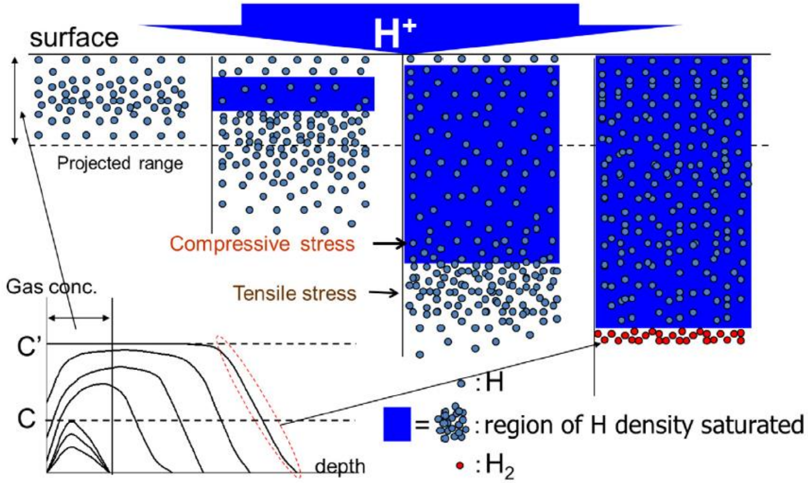

- Poly-crystalline (ITER-specification)

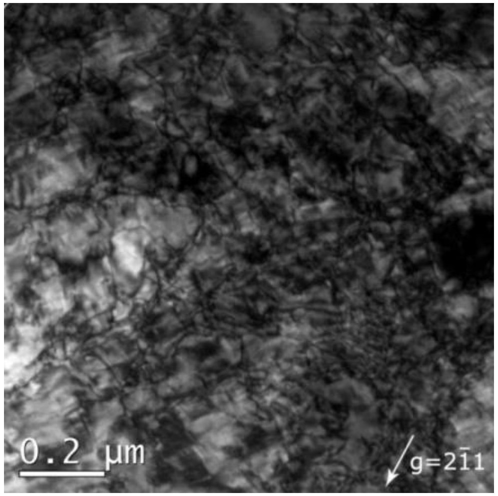

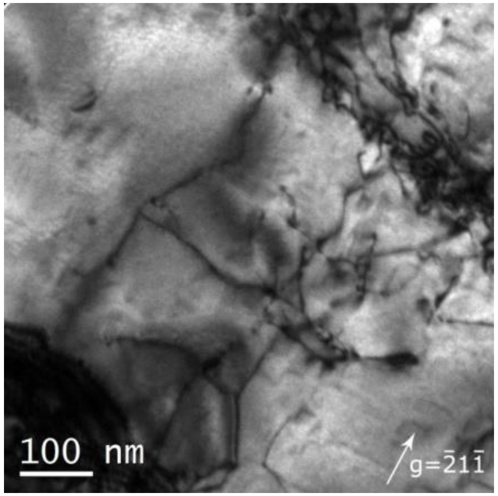

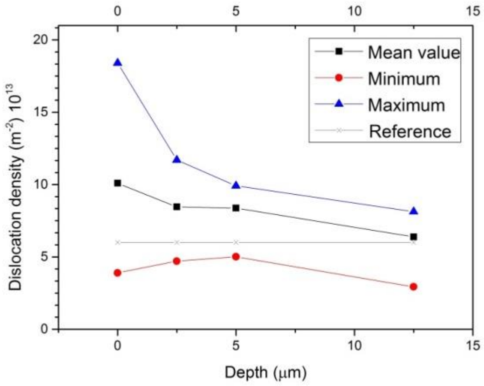

High flux plasma changes sub-surface

- Compressive stresses in sub-surface region generate:
  - Dense dislocation network
  - Limited within 10-15 μm
- Poly-crystalline (ITER-specification)
  - Recrystallized at 1600C (1h)

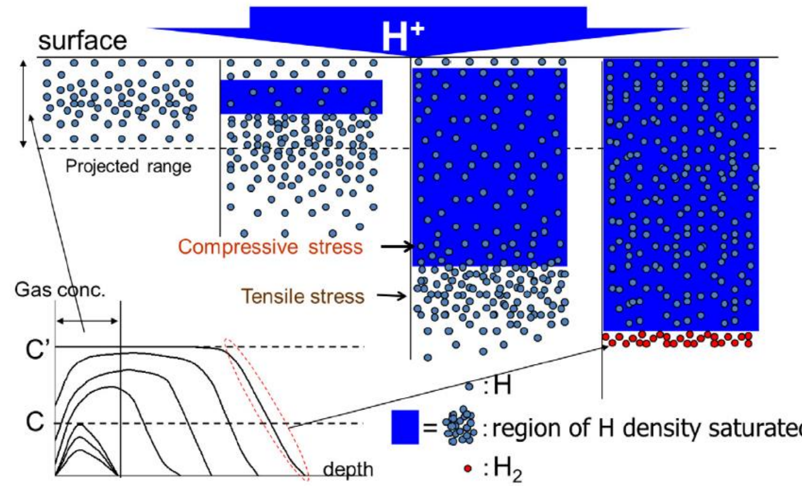

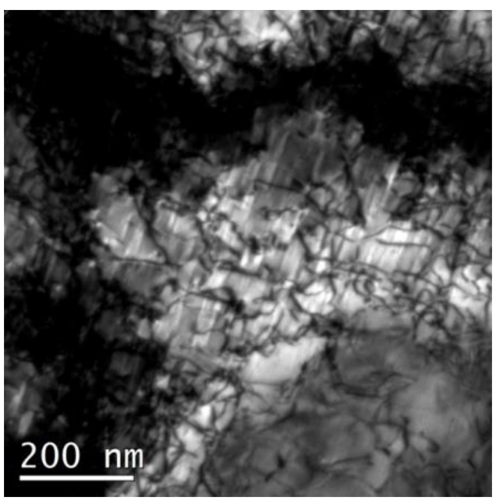

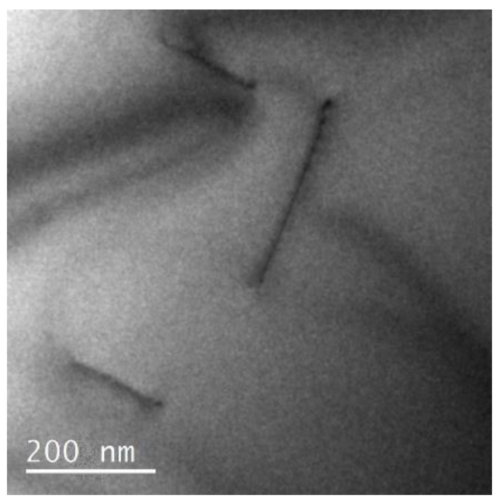

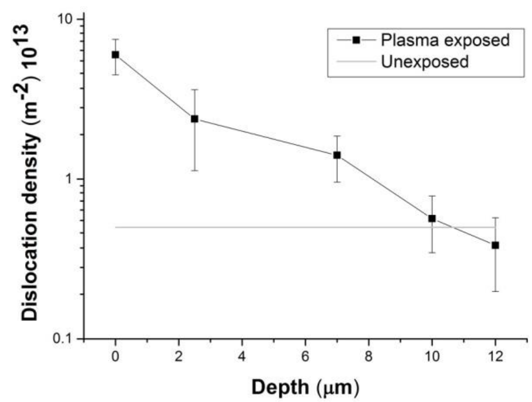

High flux plasma changes sub-surface

- Compressive stresses in sub-surface region generate:
  - Dense dislocation network
  - Limited within 10-15 μm
- Single crystal (110 orientation)

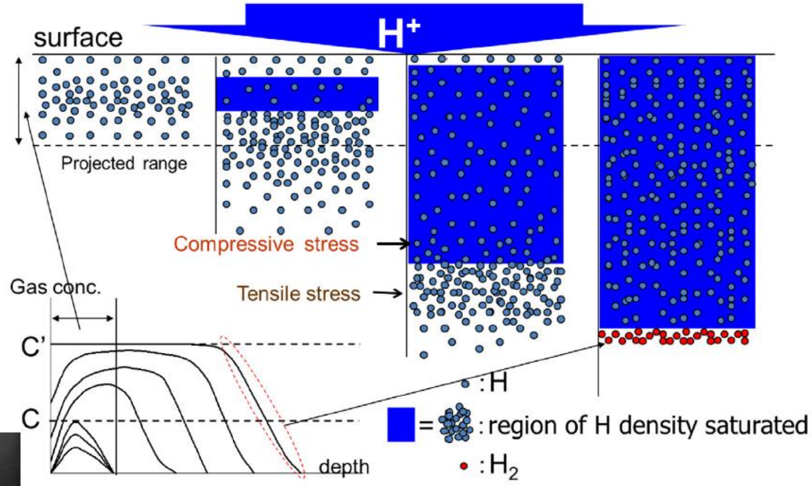

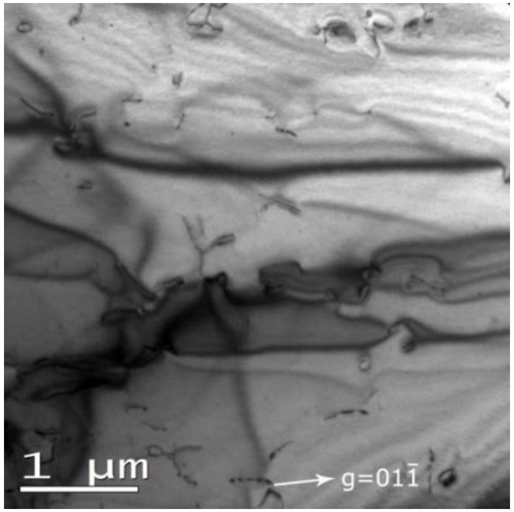

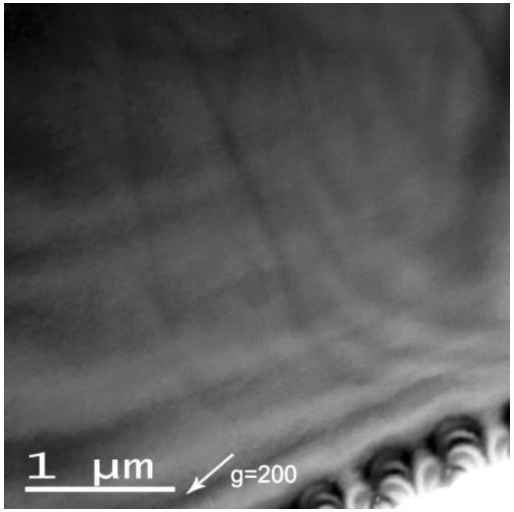

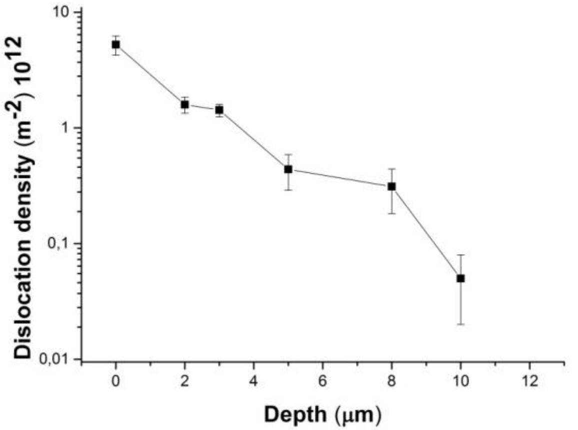

Impact of dislocation networks in pure Fe

- Plastic deformation was applied at RT up to 40%
- Grain size: 50-100 µm
- Dislocation density:
  - Non-deformed: 10^{11} m^{-2}
  - 20% - 8×10^{12} m^{-2} ; 40% - 3×10^{14} m^{-2}

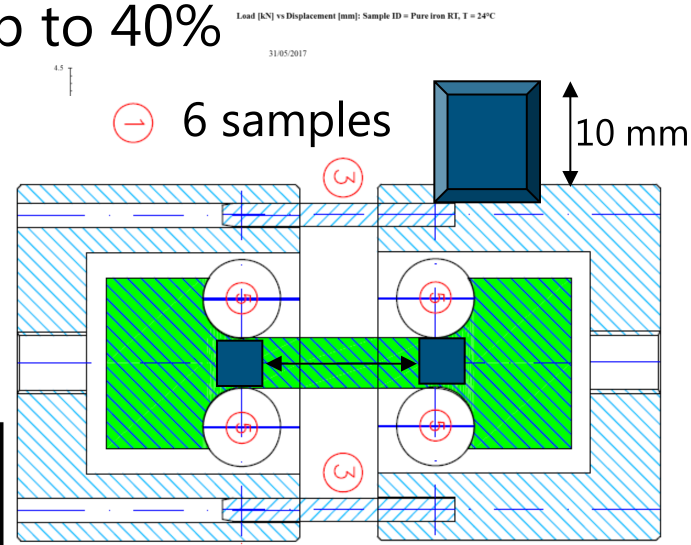

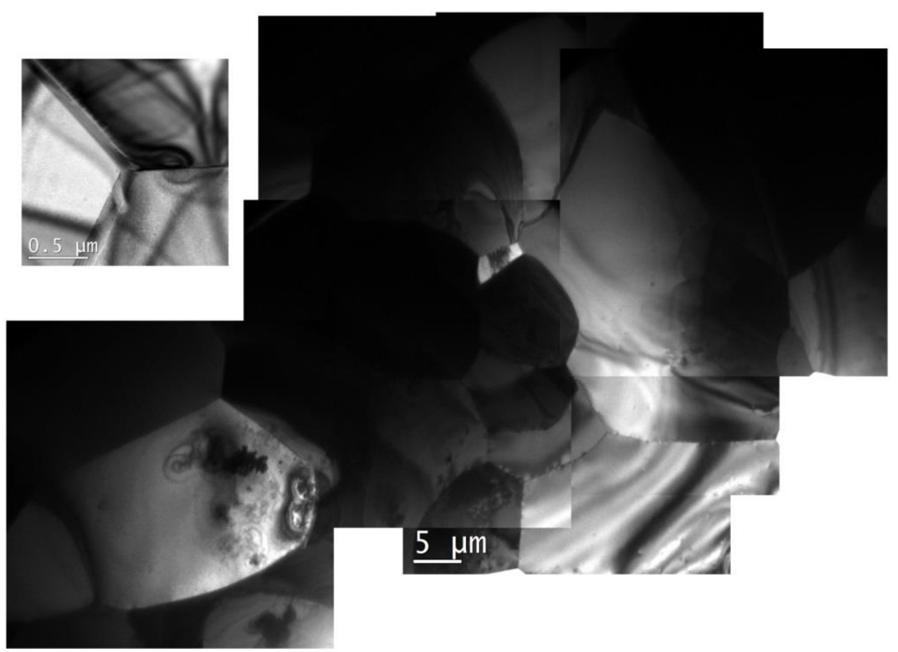

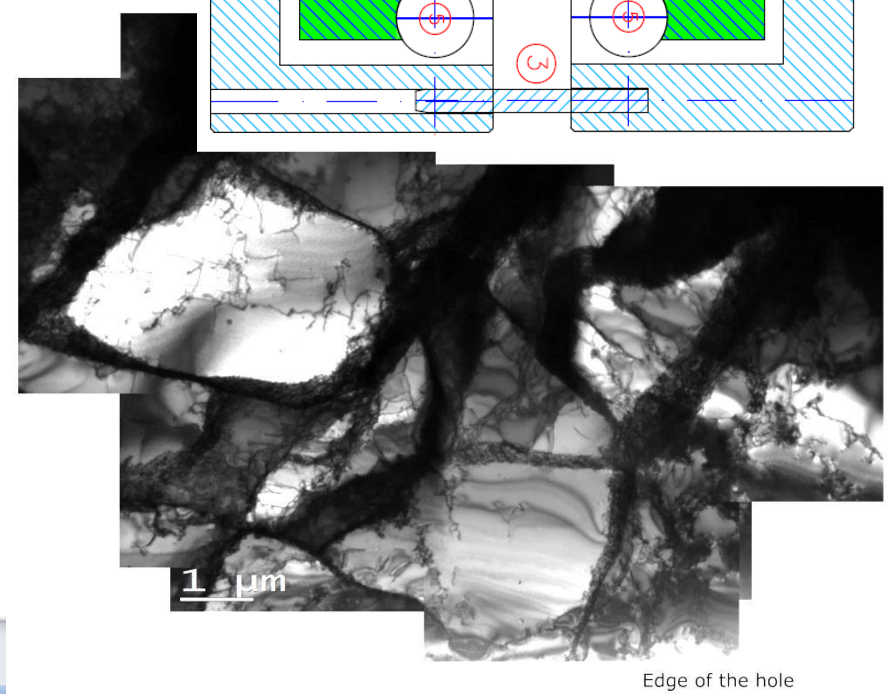

Retention in pure Fe

- High Flux D plasma exposure at Pilot PSI (NL)
  - Surface temperature: 430-450 K
  - Flux 0.8×10^{24} D/m^2/sec
  - Fluence ~5×10^{25} D/m^2

- Detrapping stages
  - Around 470K (1.2 eV)

  Position does change with increase of dislocation density
  - Around 620K (1.6 eV)

  Position shifts with increase of dislocation density

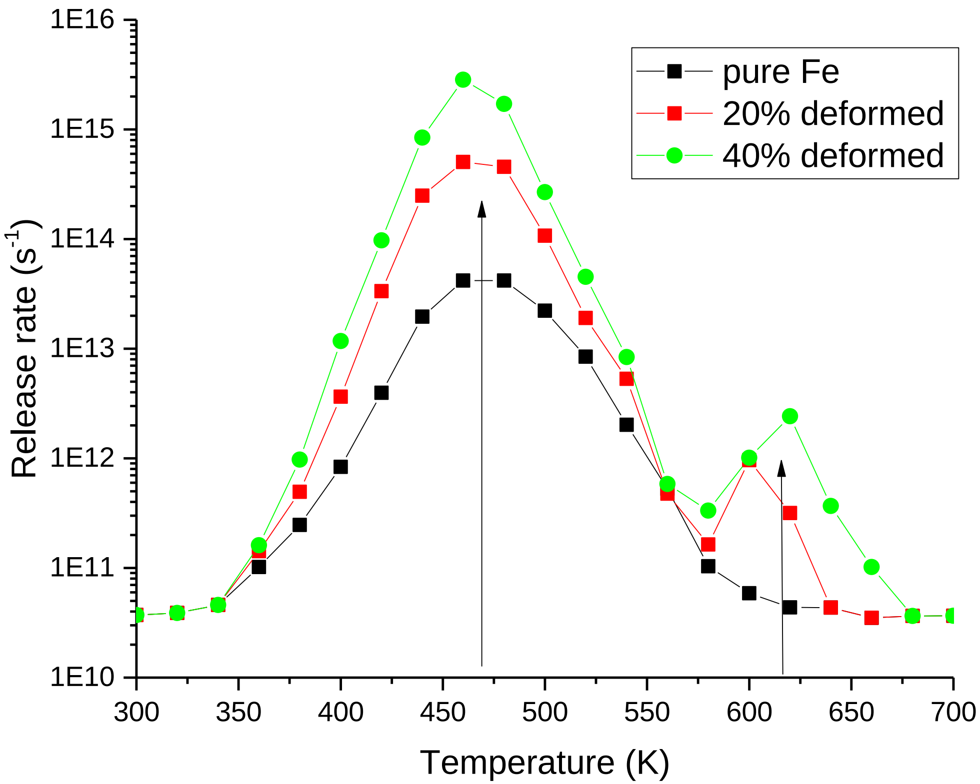

In line with results of Hong and Lee, Acta metall 32 (1984) 1581-1589

Exposure of Eurofer97 and T91

- High Flux D plasma exposure at Pilot PSI (NL)
  - Surface temperature: 430-450K
  - Flux 0.8×10^{24} D/m^2
  - Fluence ~5×10^{25} D/m^2
- Reference measurements
  - T91; E97

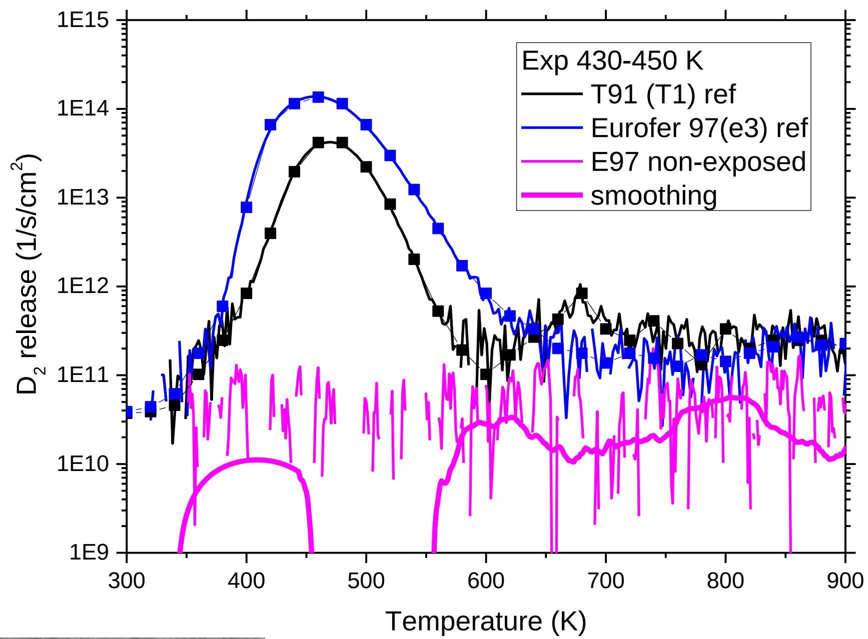

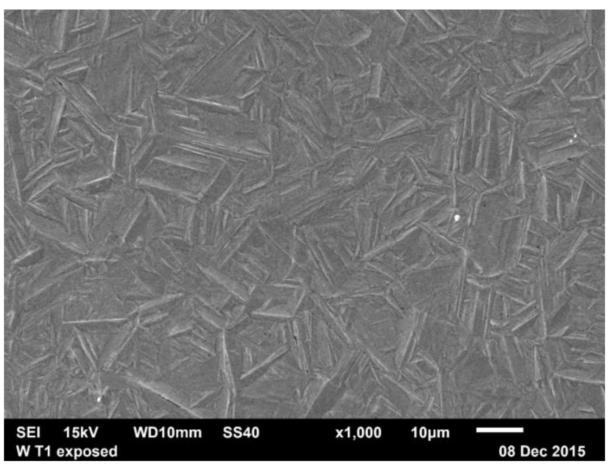

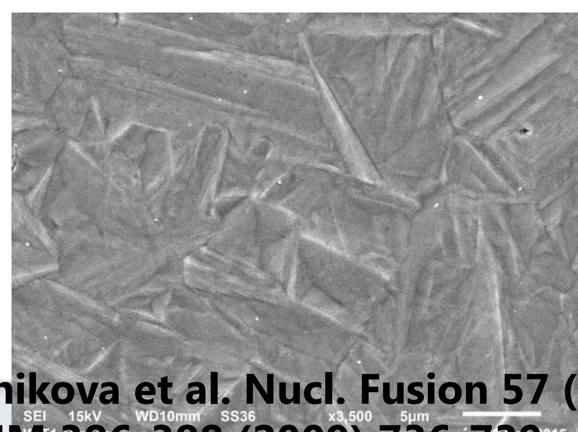

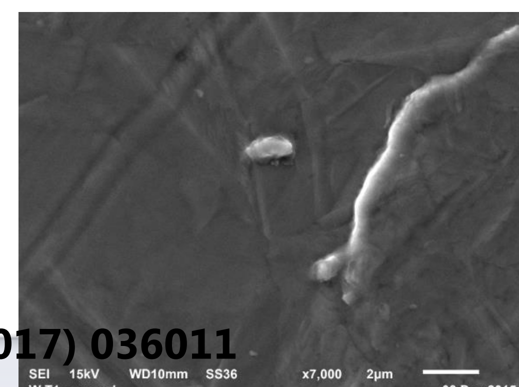

In line with results of Ogorodnikova et al. Nucl. Fusion 57 (2017) 036011 and in line with Hino et al. JNM 386-388 (2009) 736-739

Surface analysis of Eurofer97

- Exposure at 430-450K: Blisters and individual grains

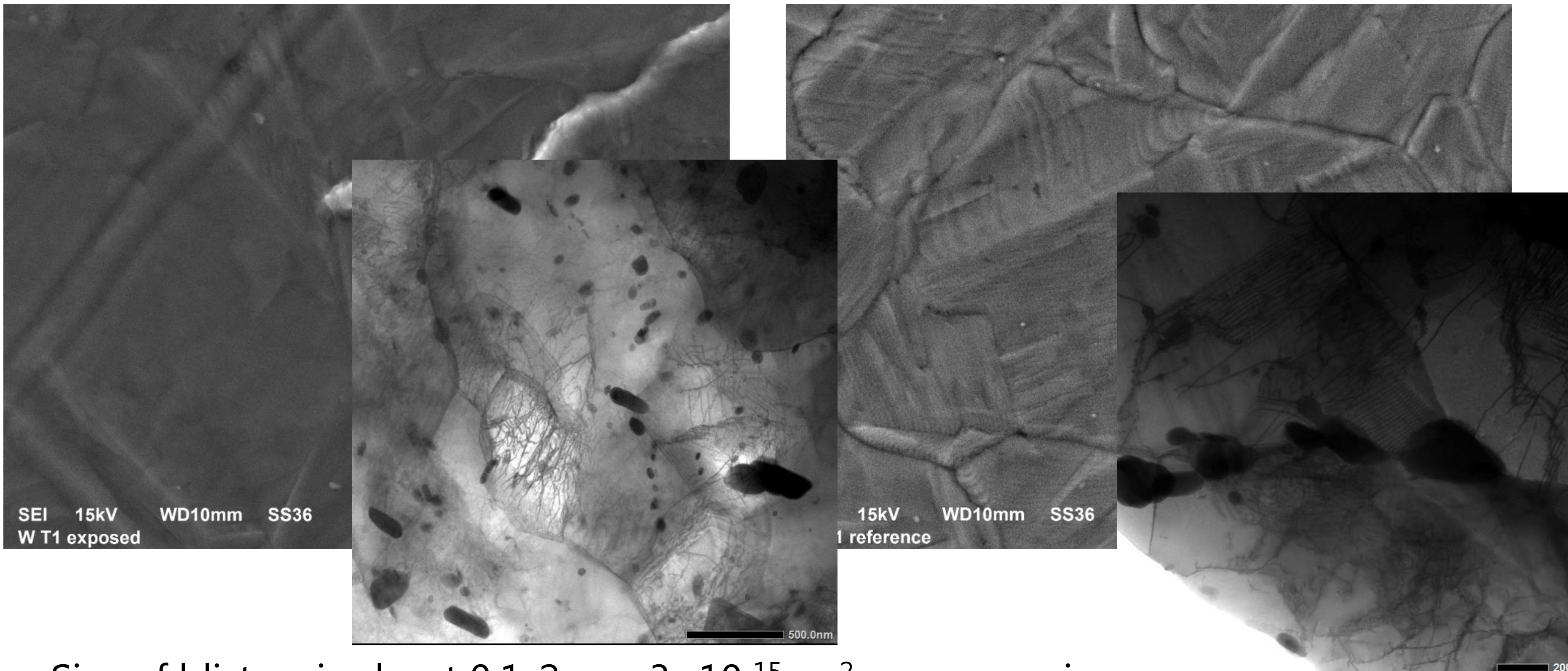

Size of blisters is about 0.1-2 μm; 3×10^{-15} m^{-2}; mean spacing 15 μm

Exposure of Eurofer97 vs. two advanced grades

- High Flux D plasma exposure at Pilot PSI (NL)
  - Surface temperature: 430-450K
  - Flux 0.8×10^{24} D/m^2
  - Fluence ~5×10^{25} D/m^2
- Release stages
  - 470K – just like in pure Fe
  - In “196C” stage at 740K

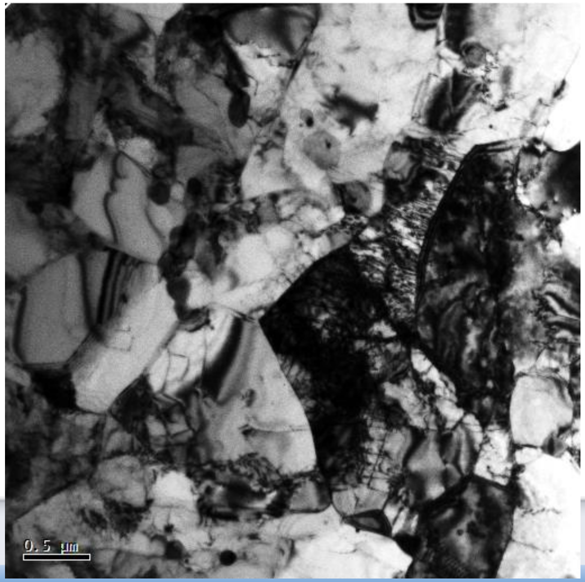

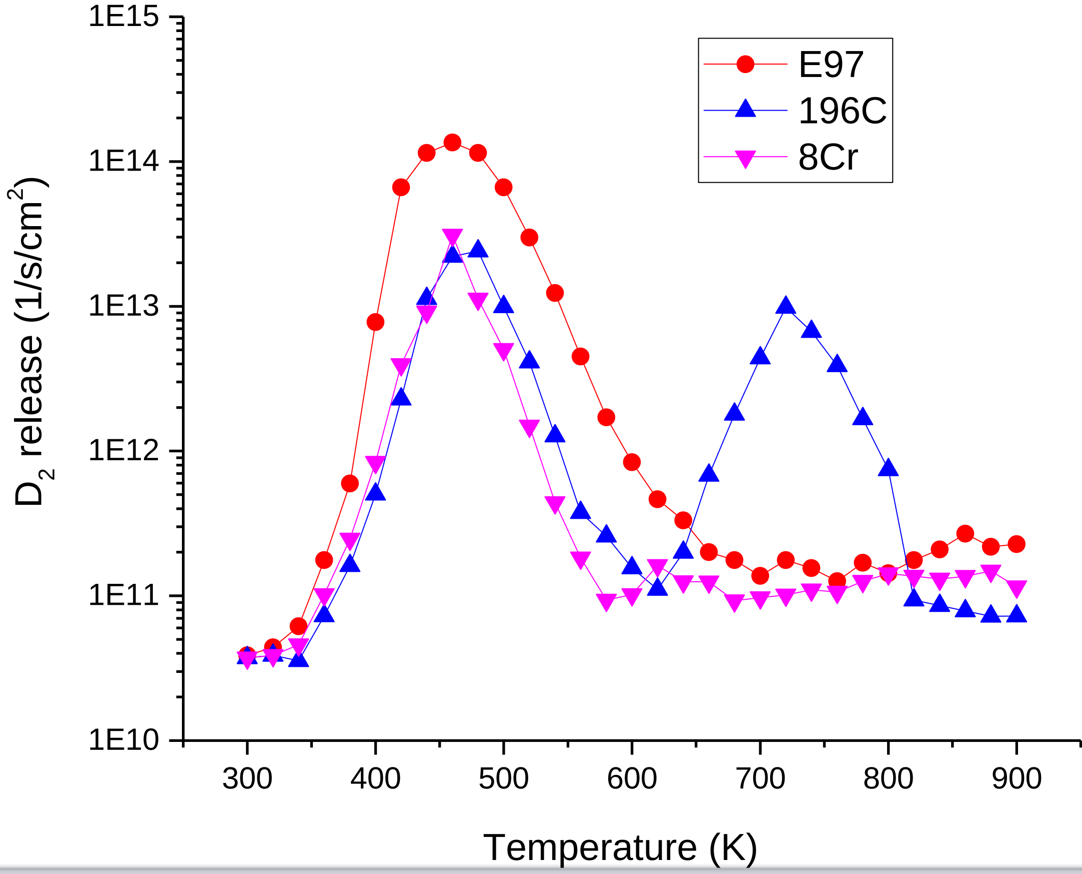

Preliminary results

- Exposure at 430-450K: E97 vs. advanced grade

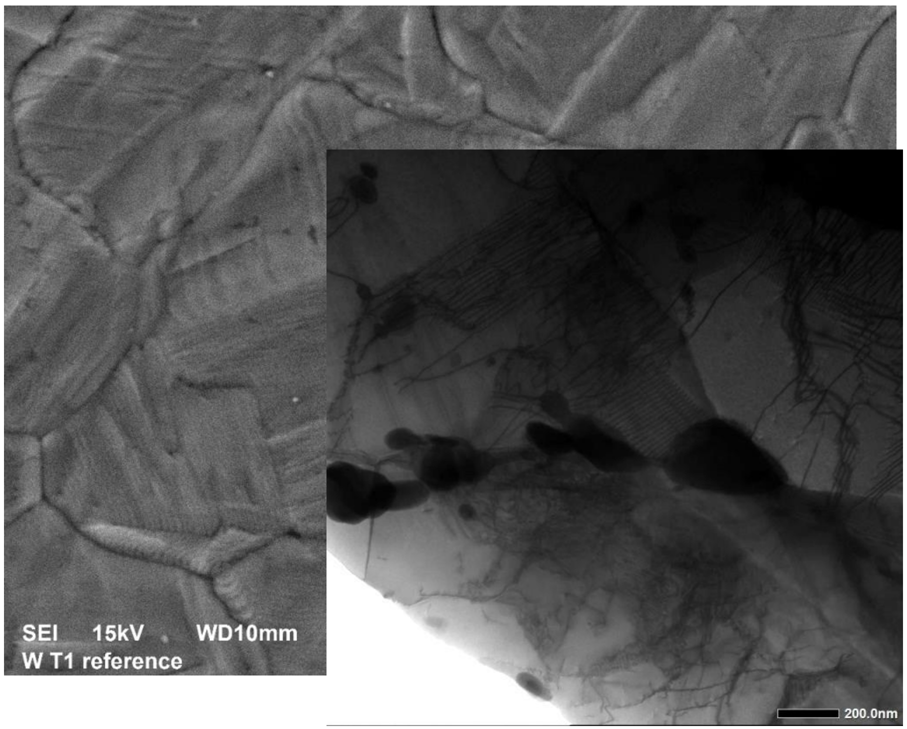

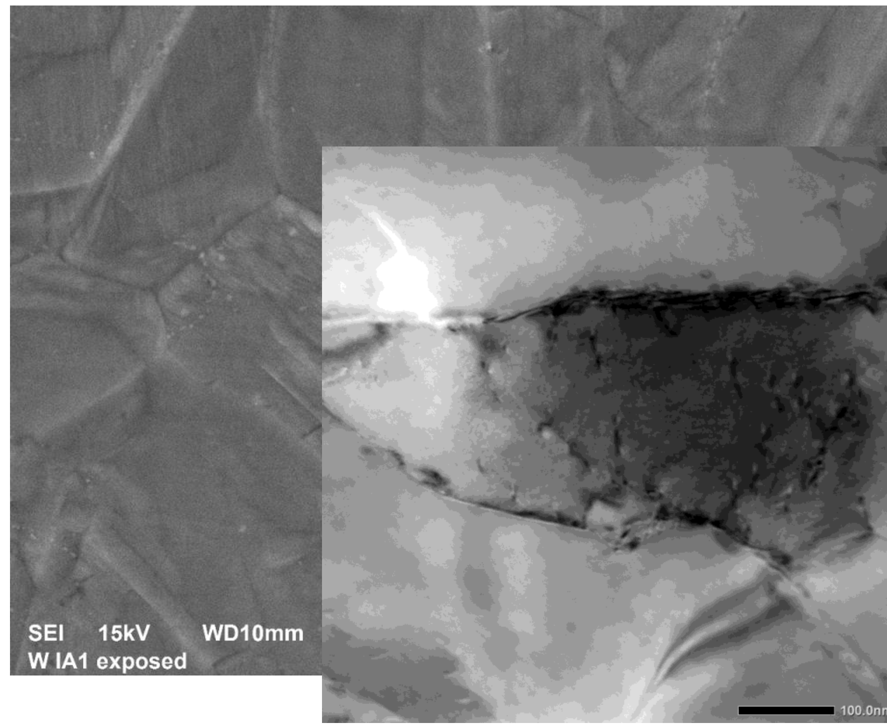

Much smaller surface roughening; lower density of blisters
Amount of plastic deformation induced in “196C” is much smaller than in E97

Summary of experimental data

- Pure Fe: one major release stage at 470K
- Plastically Deformed Fe: major release stage at 470K + emerging stage at 620K. Stage position shifts towards higher temperature with increase of dislocation density)
- E97 and T91 : spectrum is very similar to pure + minor release above 500K
- Surface microstructure of exposed steels reveals regions with very high dislocation density
- Improved RAFM steels:
  - "Clean Steel" 8Cr + 0.13Ta (no Si, Mn): spectrum same as E97
  - DBTT-optimized (0.09Ta, 880°C quenched): extra release stage at 750K. Same nature as in deformed Fe ?
  - Much smaller surface modification (higher toughness)

Part III

- Computational assessment of H in Fe

Atomic-scale description of H in bcc Fe

Vacancies   Grain boundaries

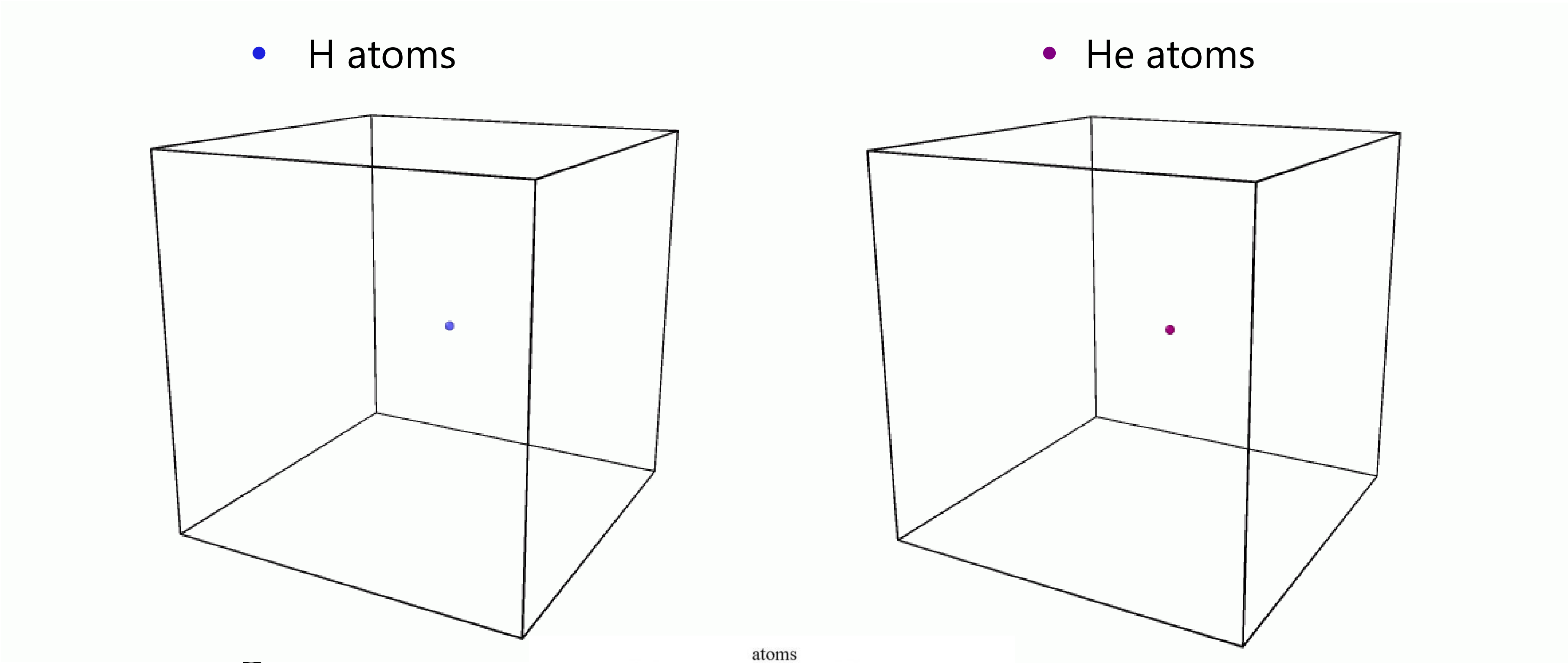

- Nucleation of stabl
  to occur on lattice

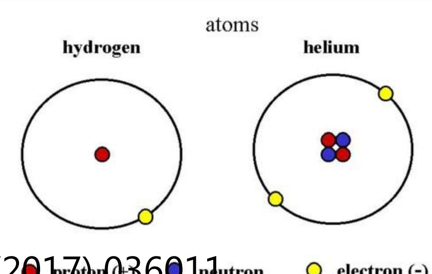

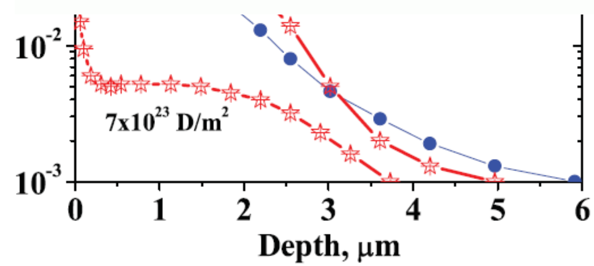

(a): Ogorodnikova et al. Nucl. Fusion 57 (2017) 036011

Hypothesis about trapping on dislocations

- Experimental and theoretical 'facts':
  - H-H can form clusters, but binding is very weak
    - Binding (H-H)=0.22 eV (A); (H_2-H)=0.08 eV (D), (H_3-H)=0.02 eV (C)
  - Migration energy = 0.09 eV
    - Diffusion of H is controlled by interaction with lattice defects
  - Typical µ-structure of RAFM steels:
    - Dislocations (10^{13}-10^{14} m^{-2})
    - Ferritic and martensitic grains, precipitates (M-X and $M_{23}C_6$)
- Possible mechanism of bubble nucleation without vacancies:

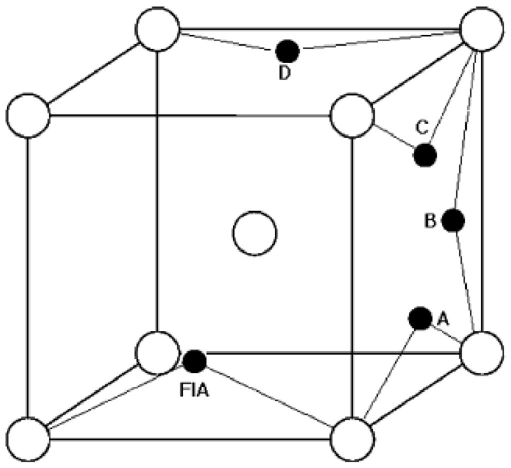

Interaction of Hydrogen with screw dislocation

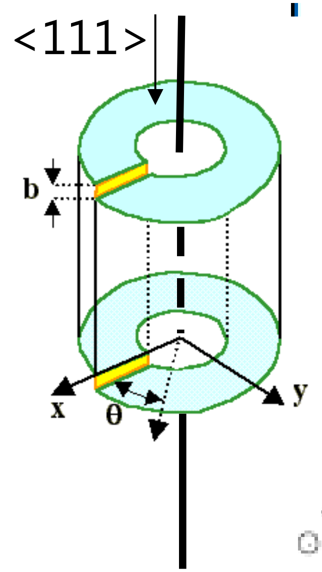

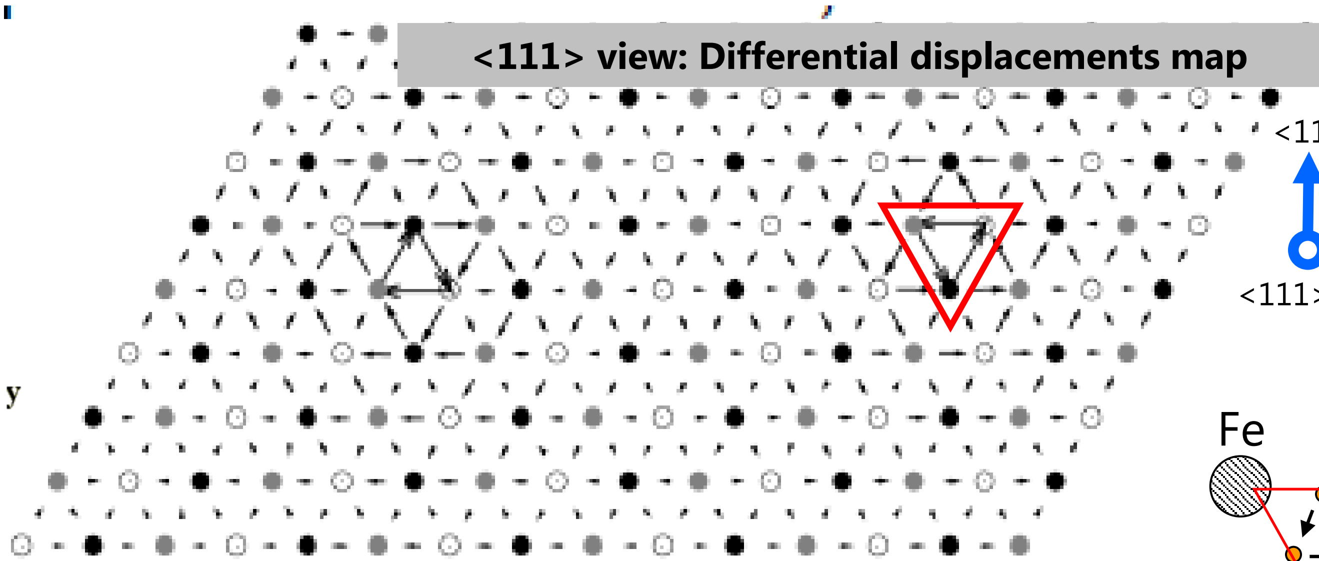

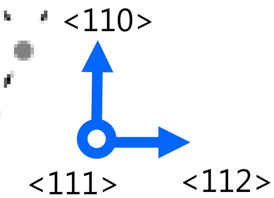

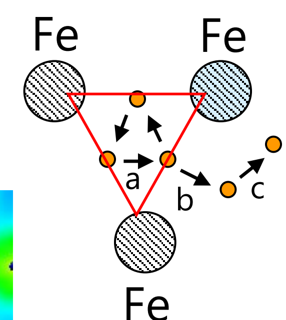

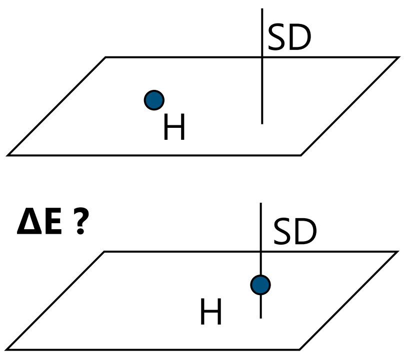

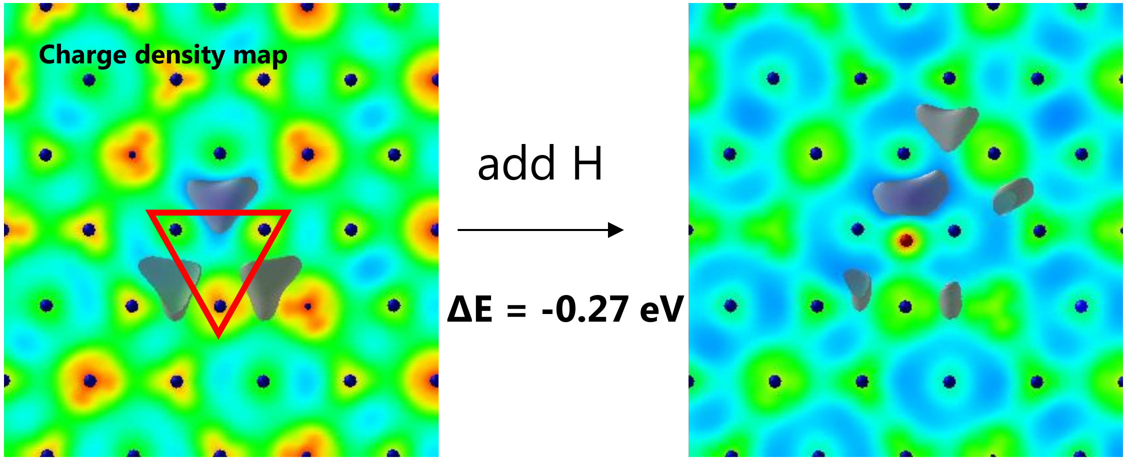

Migrations:

a – in core

b – in-out

c – out core

E_m=0.03 eV

In-pile migration of H on screw dislocation

- Migration occurs via hops through tetra-sites
- Migration barrier is 0.03 eV
- Saddle point configuration involves modification of the dislocation core structure
- Migration barrier will be strongly impacted by external stress applied

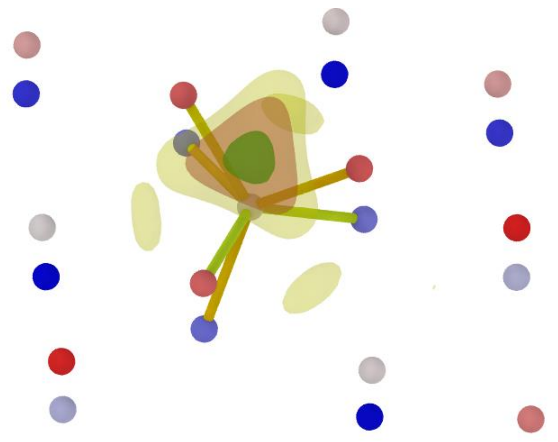

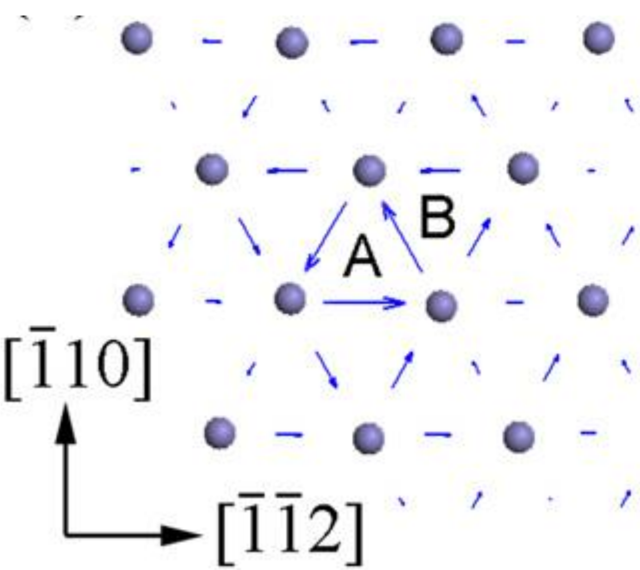

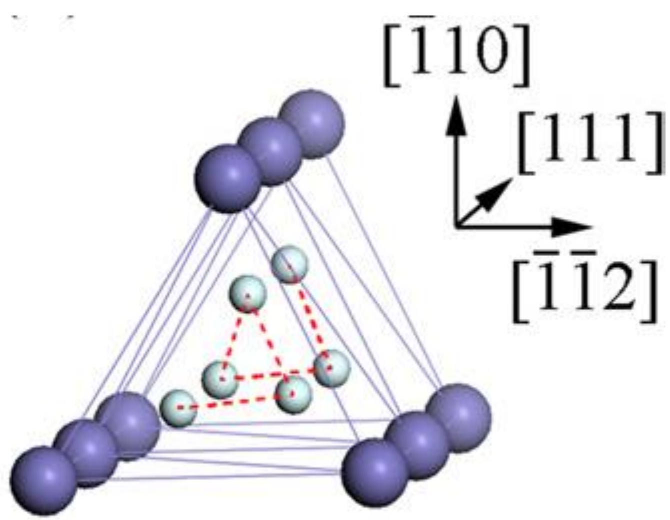

In-pile migration of H on edge dislocation

- Migration occurs via hops between tetra-sites next to the dislocation core
- Migration barrier is 0.1 eV
- Saddle point configuration is distorted octa-site

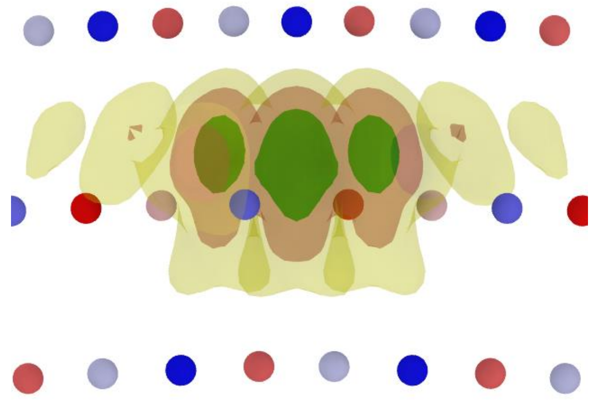

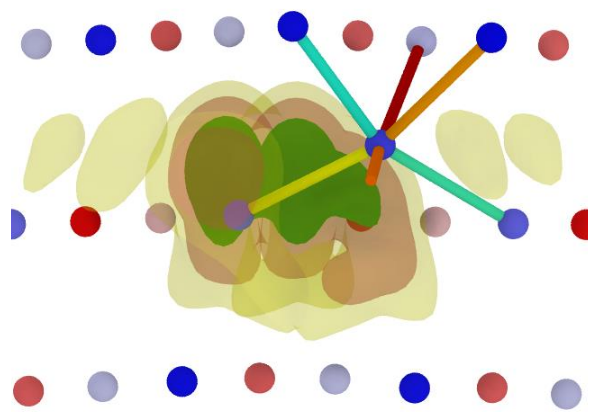

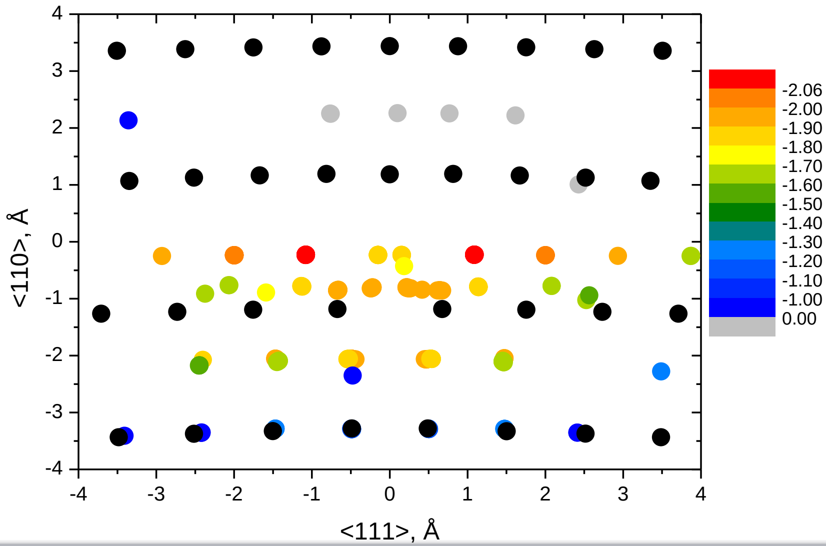

Clustering of Hydrogen on screw dislocation

Binding energy [eV]

Size of H_N cluster	SD length= 3**b**	ED Length=2.4 a_0
H + SD	0.27	0.47
H + (H-SD)	0.2	0.51
H + (H_2-SD)	0.18	0.3
H + (H_3-SD)	-0.1	0.18
H + (H_4-SD)	-0.12	0.25

Charge density maps [$e^-/Å^3$]

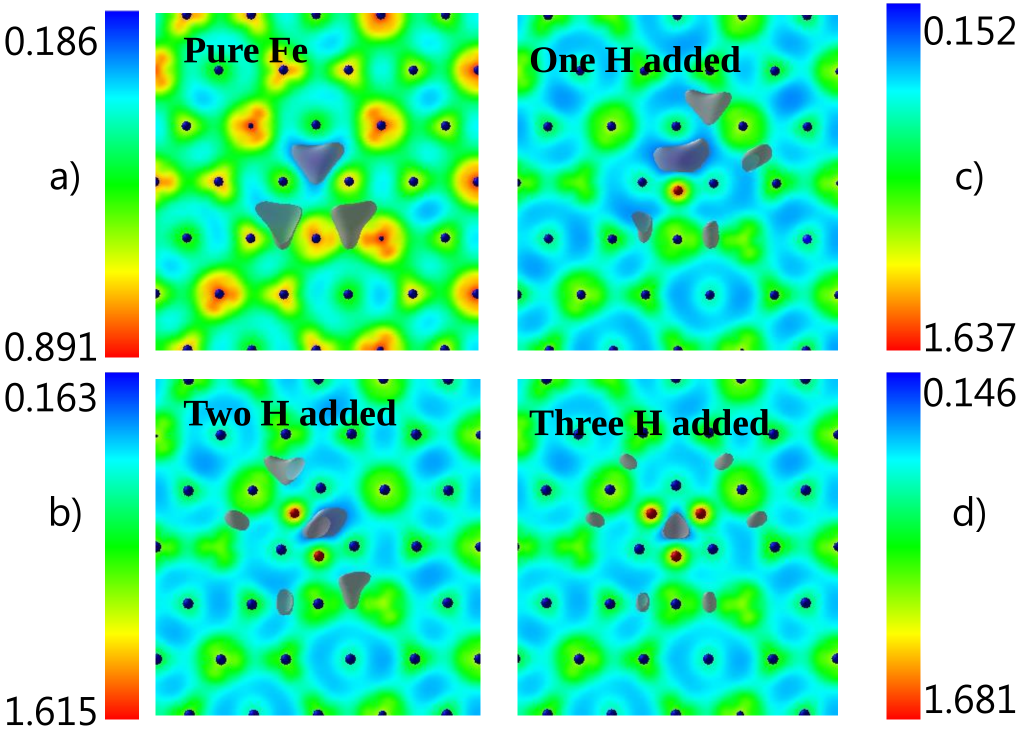

Screw dislocation can trap several hydrogen atoms simultaneously, but incremental binding energy decreases with number of trapped H atoms (from 0.27 eV– down to 0.03 eV).

Results: Molecular Dynamics Results

Validated two types of potentials EAM and BOP

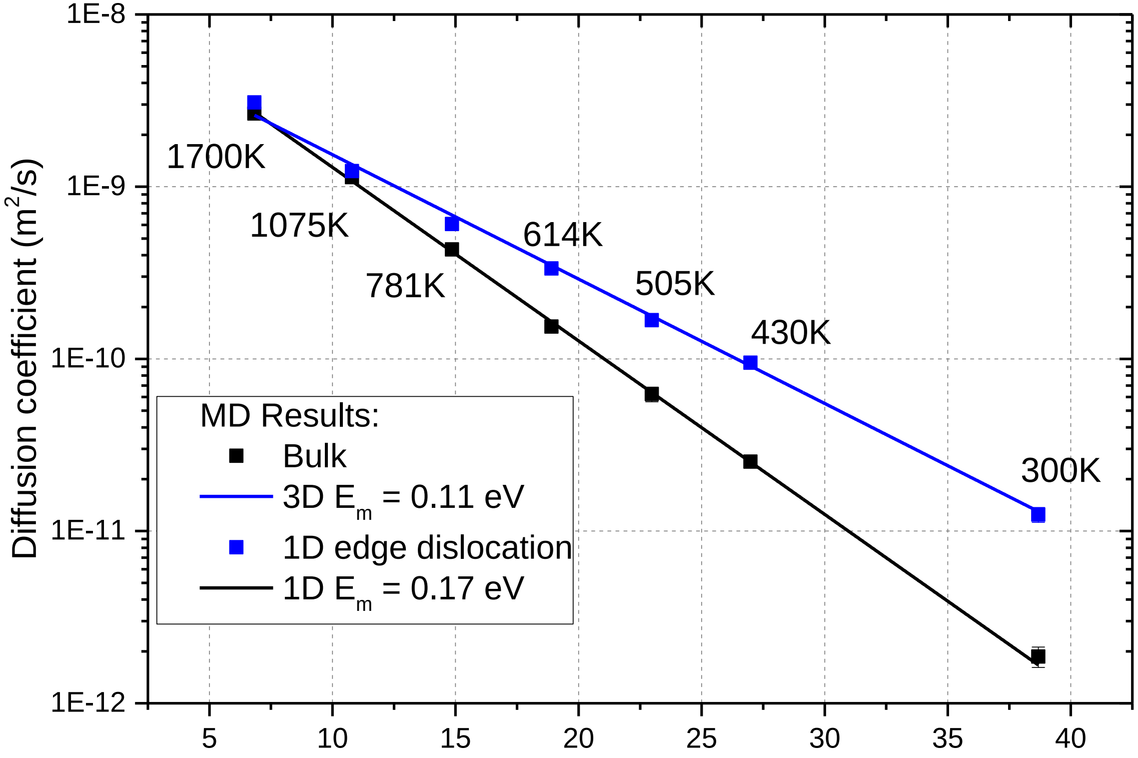

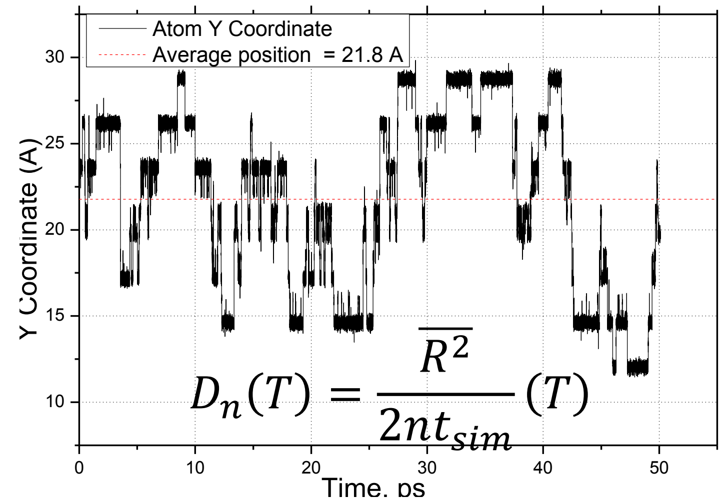

$$D_n(T) = \frac{\overline{R^2}}{2nt_{sim}}(T)$$

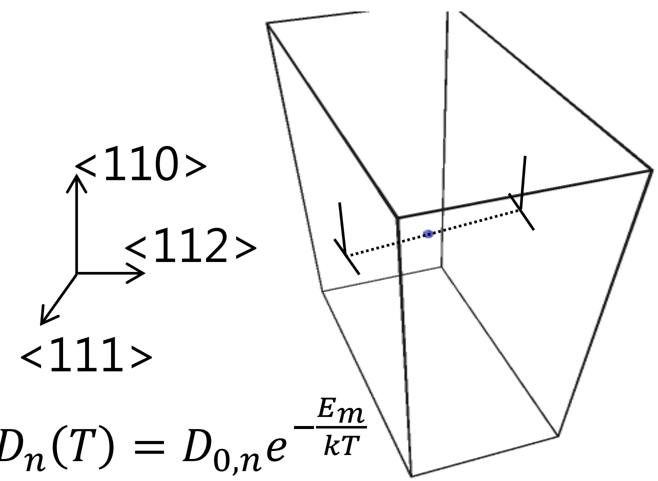

$$D_n(T) = D_{0,n}e^{-\frac{E_m}{kT}}$$

H migration at 430 K for 25 ns

Migration along the dislocation core simulated by MD reveals 0.17 eV
Hence, formation of stable H cluster must invoke some impurities to reduce the migration, for instance Carbon

Nucleation of stable Hydrogen cluster on dislocation

Loop punching: growth of bubbles due to excess pressure via the emission of dislocation loops

A: Dislocation + cluster H_N

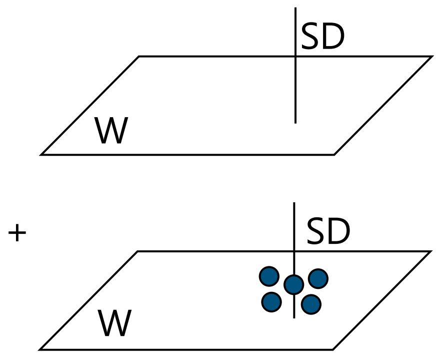

B: dislocation + (**Jog**—H_N) + **Jog**$^+$

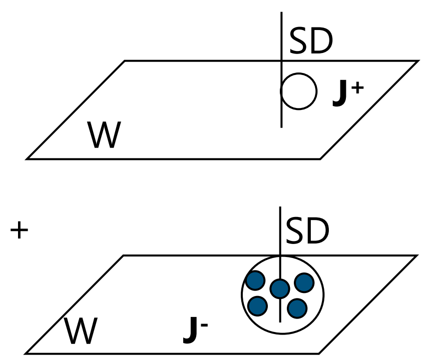

Classical loop punching mechanism

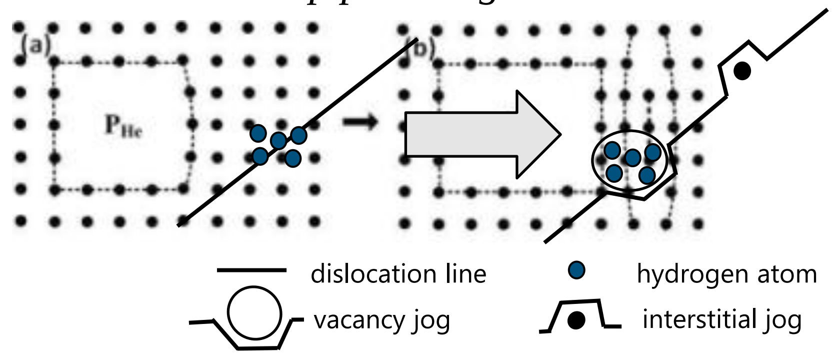

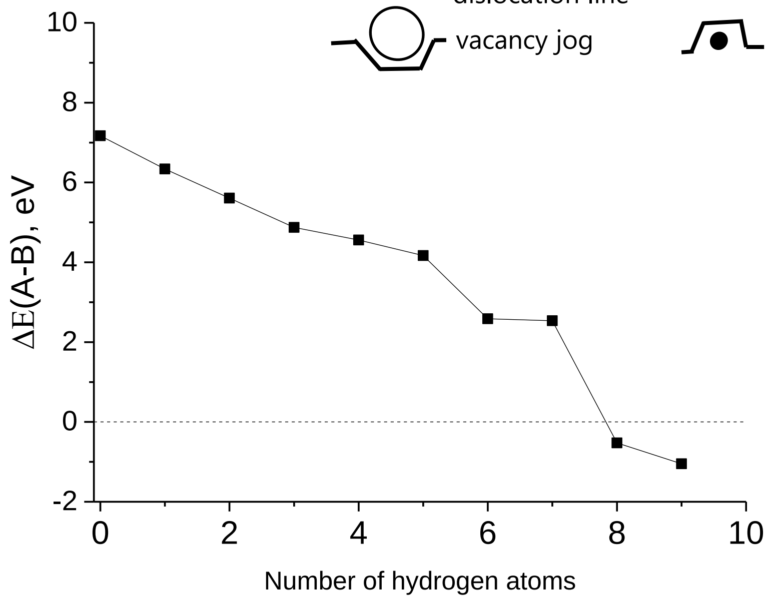

No attraction of H in bulk – no way to form critical concentration.

Clustering at dislocation core leads to jog emission at N_H=8

Jog punching: formation of vacancy jog to accommodate H_N cluster + emission of interstitial jog

Nucleation of stable Hydrogen cluster on dislocation

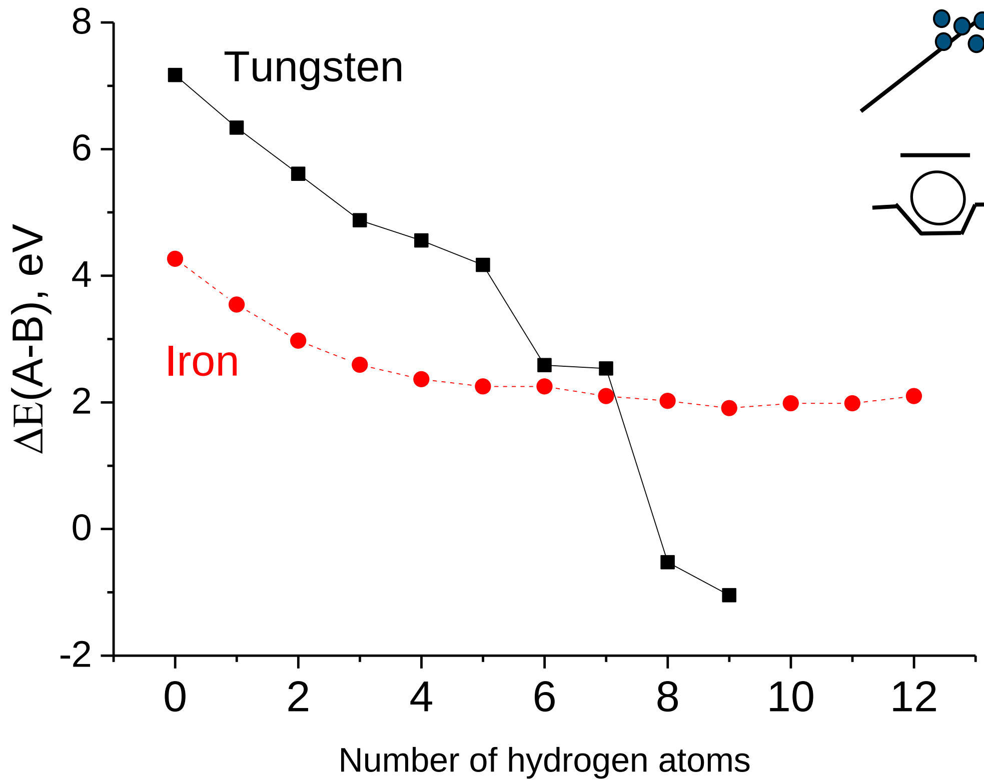

Jog emission mechanism

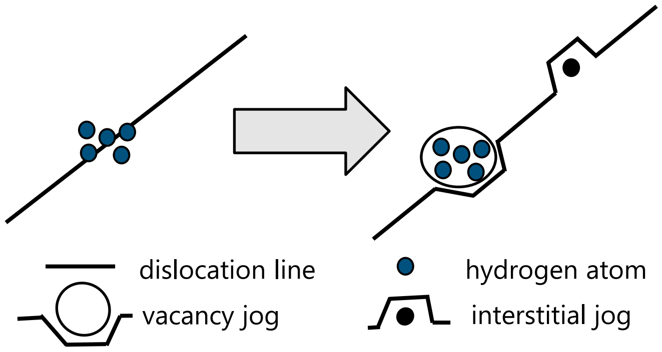

Because of the negative solution energy, H clusters can not induce jog punching

Jog punching: formation of vacancy jog to accommodate H_N cluster + emission of interstitial jog

Nucleation of stable Hydrogen cluster on dislocation

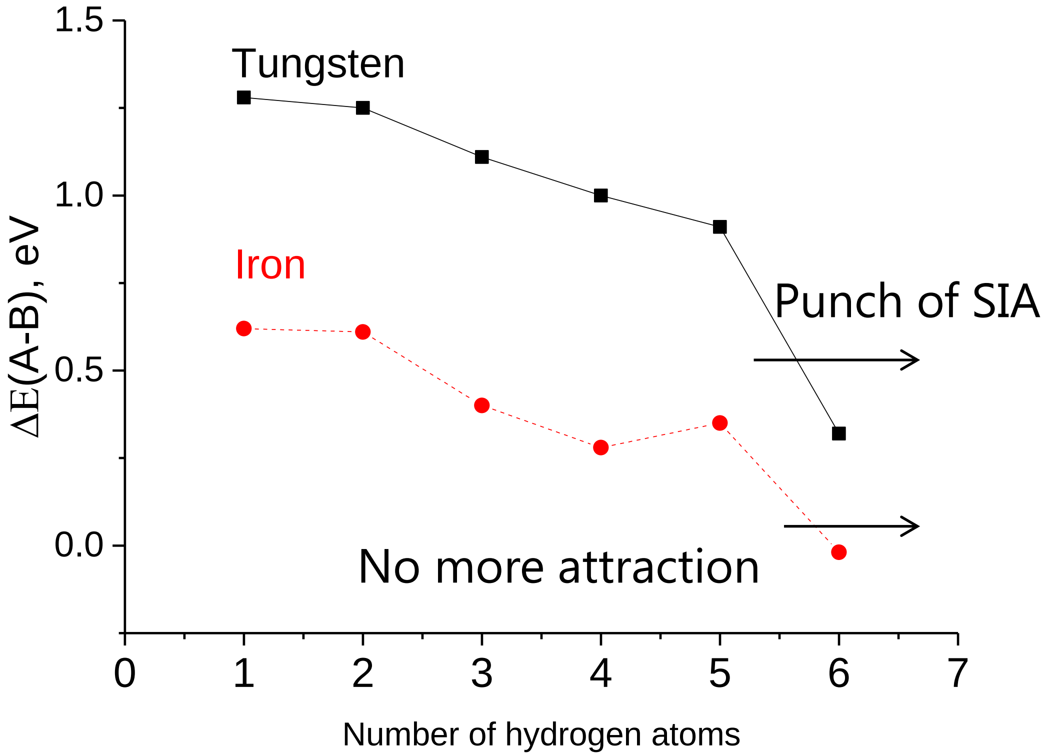

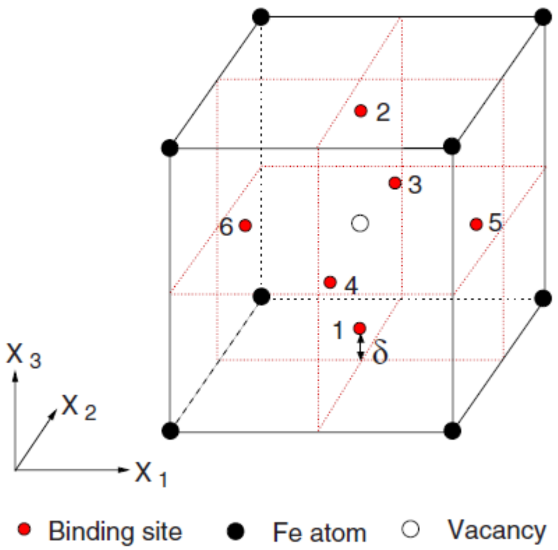

Because of the negative solution energy, H clusters can not induce SIA emission

Jog punching: formation of vacancy jog to accommodate H_N cluster + emission of interstitial jog

Summary of atomic-scale data for H in Fe

- H solution energy -2.33 (H adds to cohesion of Fe) – tetra-site
- H-H binding in Fe 0.22 eV, and it reduces to 0.02 eV for H_3-H cluster
- H-vacancy binding 0.62 eV; one vacancy accepts 5 H atoms and does not growth further by emission of SIAs
- H-dislocation binding 0.27 eV and 0.47 eV (SD & ED); jog-emission is not energetically favourable mechanism
- H migration energy in bulk = 0.09 eV from tetra-to-tetra site;
- H migration energy on screw dislocation = 0.05 eV;
- H migration energy on edge dislocation = 0.1 eV

- Formation and growth of H defects resulting in blisters could be related to:
  - Nucleation of flake-like H clusters at GB interfaces, Carbide-GB interfaces
  - Growth of those defects by loop emission (as availability of H promotes plastic deformation)

Description of the model

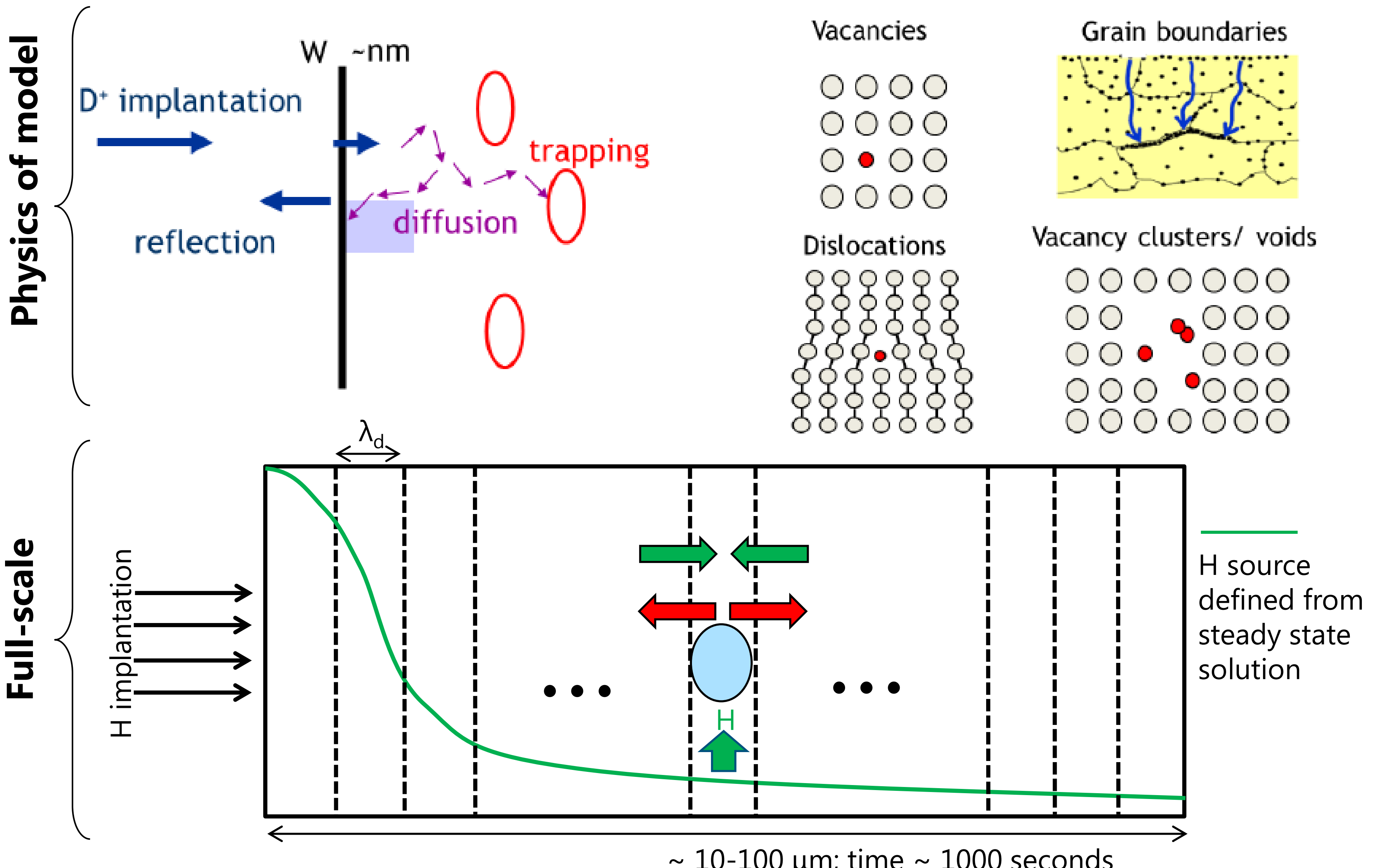

outlook

- Complete computational model
  - Assess formation of H clusters at grain boundaries and Carbide-Fe interfaces
  - Assess interaction of H-vacancy-Carbon defects
- Parametric study of the high flux plasma exposure
  - Exposure temperature : 450K – 850K (upper limit for RAFM)
  - Exposure dose : $5\times10^{25} – 10^{27}$ D/m^2
  - Materials: Fe, Plastically deformed Fe; Eurofer97; “Clean Steel” (no Si & Mn)

Spare slides

Preliminary results

- High Flux D plasma exposure at Pilot PSI (NL)
  - Surface temperature: 950-970 K
  - Flux ~10^{24} D/m^2
  - Fluence ~5×10^{25} D/m^2
- Reference measurements
  - E97;